sustainability

MDPI

Article

A Multi-Criteria Decision Maker for Grid-Connected Hybrid Renewable Energy Systems Selection Using Multi-Objective Particle Swarm Optimization

David Abdul Konneh [1,*], Harun Or Rashid Howlader [1], Ryuto Shigenobu [1], Tomonobu Senjyu [1], Shantanu Chakraborty [2] and Narayanan Krishna [3]

1 Department of Electrical and Electronics Engineering, University of the Ryukyus, Okinawa 903-0213, Japan; h.h.howlader@ieee.org (H.O.R.H.); e115562lute@gmail.com (R.S.); b985542@tec.u-ryukyu.ac.jp (T.S.)
2 Energy Transition Hub, University of Melbourne, Melbourne 3053, Australia; shantanu.chakraborty@unimelb.edu.au
3 Department of Electrical and Electronics Engineering, SASTRA Deemed University, Thanjavur-613401, India; narayanan@eee.sastra.edu
* Correspondence: davidulkon@gmail.com

Received: 11 January 2019; Accepted: 18 February 2019; Published: 23 February 2019

Abstract: Combating climate change issues resulting from excessive use of fossil fuels comes with huge initial costs, thereby posing difficult challenges for the least developed countries in Sub-Saharan Africa (SSA) to invest in renewable energy alternatives, especially with rapid industrialization. However, designing renewable energy systems usually hinges on different economic and environmental criteria. This paper used the Multi-Objective Particle Swarm Optimization (MOPSO) technique to optimally size ten grid-connected hybrid blocks selected amongst Photo-Voltaic (PV) panels, onshore wind turbines, biomass combustion plant using sugarcane bagasse, Battery Energy Storage System (BESS), and Diesel Generation (DG) system as backup power, to reduce the supply deficit in Sierra Leone. Resource assessment using well-known methods was done for PV, wind, and biomass for proposed plant sites in Kabala District in Northern and Kenema District in Southern Sierra Leone. Long term analysis was done for the ten hybrid blocks projected over 20 years whilst ensuring the following objectives: minimizing the Deficiency of Power Supply Probability (DPSP), Diesel Energy Fraction (DEF), Life Cycle Costs (LCC), and carbon dioxide (CO_2) emissions. Capacity factors of 27.41% and 31.6% obtained for PV and wind, respectively, indicate that Kabala district is the most feasible location for PV and wind farm installations. The optimum results obtained are compared across selected blocks for DPSP values of 0–50% to determine the most economical and environmentally friendly alternative that policy makers in Sierra Leone and the region could apply to similar cases.

Keywords: wind energy; solar energy; biomass energy; battery energy storage; grid-connected hybrid energy system; diesel energy fraction; CO_2 emissions; reliability and sustainability; MOPSO

1. Introduction

Energy is an essential component in the development of any society. The understanding of this fundamental principle is deeply embedded in the United Nations Sustainable Development Goal 7 (UNSDG7) [1], which clearly emphasizes universal access to affordable, reliable, and modern energy services, whilst increasing substantially the share of renewable energy in the global energy mix by 2030. Whilst some countries are taking leading roles in meeting this agenda, most countries in Sub-Saharan Africa (SSA) have been snail paced. The region still has the lowest household electrification rate worldwide, with about 588 million people living without (2016 report) [2]. Though Sierra Leone,

a small country located along the Atlantic Ocean in West Africa, has a small population of about 7 million, the daily power delivery is not guaranteed and is currently far below the overall demand. The obligation of the Ministry of Energy (MoE) to provide sustainable electricity for its citizens over the past decades has been met with several obstacles including the civil war (1991–2001) leading to vandalizing existing energy infrastructure, crippling management systems, and minimum funds to invest in renewable energy technologies. This leaves the current access to electricity to be barely 15% with about 3% rural access, which is well below the current average in SSA. Political will and economic instability have been driving factors limiting governments from investing in state of the art technologies. The unemployment rate is high (4.5%) [3] for a country with a very small population and an electricity tariff of 18.76 USc/kWh, sitting amongst the highest in region, making electricity less affordable to the poor. These measures are in complete disagreement with the UNSDG7 agenda. Irrespective of other domestic and international factors, lack of electricity access has influenced to a great extent the snail paced growth of private sector investment.

At the moment, desperate but uneconomical and unsustainable measures are being adopted by governments in trying to meet the unsuppressed national demand of about 700 MW, inclusive of existing and projected demand of mining companies and new settlements across the country. However, these measures are taken with little concern for the environment as more rental power with diesel generation is been injected to close the gap between generation and demand. According to the Sustainable Energy for All (SE4ALL) initiative launched in 2012, the target trajectory for Sierra Leone requires increasing electricity access from 15% to 92% by 2030 [4]. This would require considerably improving the share of renewable energy technologies to meet the demand in order to minimize the current burden on the government to heavily subsidize the current cost of electricity at a rate of 0.15 US$/kWh for private residents and 0.26 US$/kWh for industry. Albeit the potentials of Solar (1600 kWh/m^2/year) or an estimated 2180 h of sunshine, hydro (about 2000 MW for 27 sites), and biomass, about 2000 GWh/year, the total installed government owned generation capacity is about 130 MW, and another operational 50 MW rental power from an Independent Power Producer (IPP). Subscribing to IPPs running on diesel engines usually comes with high tariffs and this accounts for very high operational costs owing to high and fluctuating fuel costs. For the government-owned diesel plants, a huge percentage of the total revenue collected is utilized for the purchase of imported heavy fuel oil and diesel oil to run the plants, especially during the dry season. This causes the government to heavily subsidize the electricity generation. It is against this backdrop that this research has been undertaken.

Many authors have done work on hybrid energy systems ranging from residential, institutional, industrial, off-grid to grid applications. Renewable Distributed Generations (RDGs) are essential in power systems as they provide energy security and reduce power losses whilst increasing the overall efficiency and environmental protection [5]. However, renewable energy sources are stochastic in nature and thus the application of hybrid energy systems is essential in overcoming the weaknesses of stochasticity with the strength of the other, or predictability of a conventional technology [6]. Literature [7] analyzed four different hybrid energy options to reduce overall energy consumption and CO_2 emissions from residential sector. The authors in [8] presented the possibility of integrating a grid-connected renewable energy system to meet the energy demand of institutional buildings for an Indian scenario. Additionally, the authors employed a modern approach based on the Analytic Hierarchy Process for the optimum planning of the electric power system. Establishing standard methodologies to integrate RDGs to overcome today's challenges towards sustainable development is crucial and very complicated. Literature [9] examined the use of multi-criteria decision making methods for ranking three subcidy schemes of grid-connected and autonomous solar Photo-Voltaic (PV) technologies, for promoting PV systems in Cyprus. An optimization based on techno-economic analysis of grid-connected hybrid systems was done also in India, with comparison of three different scenarios based on per unit cost of electricity production, cost of operating diesel generator, and minimization of Green House Gases (GHG) [10]. The authors in [11] optimally sized stand-alone and

grid-connected PV technology for a case in Australia, whilst comparing with the optimized model of Diesel Generation (DG) system. The literature used the basis of economic feasibility and environmental impact anlysis to compare the optimized models. Resource assessment and techno-economic analysis of Hybrid Energy systems (HES) has been done with a case study approach in Saudi Arabia [12]. The authors did resource assessments for wind and PV technologies to determine their technical and economic feasibility for four cities in Saudi Arabia and achieved a reduction of energy costs and GHG emissions. Reference [13] carried out resource assessments using similar approaches in Nigeria, a case study in SSA. Literature [14] carried out an assessment of grid-connected PV and Biomass energy system to provide electricity for rural communities in Egypt. The results obtained revealed that the hybrid renewable energy system proves efficient for emissions and cost reductions. However, with the exception of assessments done by Japanese International Cooperation Agency (JICA), World Bank, and other donor organizations, no academic research has been carried out on both resource assessment and techno-economic analysis of grid-connected systems in Sierra Leone. Additionally, from the database of similar work done on multi-criteria analysis for grid-connected systems, no work has been done considering resource assessments and analysis of ten different hybrid considerations for five different technologies. Therefore the novelty of this research stems from this background with focus on the Sierra Leone scenario, whilst establishing practical boundary conditions on the resources based on the results obtained from the resource assessments. In most engineering problems the established multiple objectives are often conflicting which implies any improvement in one leads to a suppression of the other. Therefore establishing a trade-off between different objectives give rise to different solutions. Several researchers have used different tools for integration of renewable resources, like the Holistic Grid Resource Integration and Development (HiGRID) tool [15] and HOMER simulator [16]. The literature [17] examines dynamic operation and control strategies for a microgrid hybrid energy system and applied Particle Swarm Optimization (PSO) algorithm to analyze the performance of the PV power system. The authors in literature [5] applied a hybrid PSO and Gravitational Search Algorithm (PSOGSA) to deduce the optimum location of PV and wind systems for minimizing system power losses and operating costs whilst improving voltage profile and stability. Genetic algorithm (GA) was used to optimally size a PV hybrid renewable energy system in [18] with the objective of decreasing operation costs and emission of pollutants. MOPSO has been used in this study to optimally minimize the DEF, DPSP, LCC, and CO_2 emissions.

In general, the PSO algorithm performs very well with higher scale or as the problem becomes complex. Using evolutionary algorithms, such as Non-dominated Sorting Genetic Algorithm (NSGA-II), are usually computationally expensive in that the crowding distance works in the objective space only [19]. In addition to its speed of convergence and ease of application requiring the use of simple operation of real numbers, MOPSO does not require sorting of fitness values of solutions in any process. It uses leaders or region based selection instead of individuals within the search space to guide the search. Hence, this presents a significant computational advantage as the size gets larger [20]. Ting LI et al. elaborated on the methodology of the standard MOPSO algorithm and presented a comprehensive survey whilst listing references on its applications in power systems economic dispatch including Economic Environmental Dispatch (EED) and multi-area EED [21]. The authors further highlighted the advantages of MOPSO over other optimization methods. However, it is worth noting that MOPSO has computational limitations of handling constraints and the static analysis of tradeoffs. WL Theo et al. [22], also presented a review on system planning and optimization techniques applicable to hybrid energy systems integration whilst comparing various mathematical programming methods. Reference [23] used MOPSO algorithm to compute sufficient capacity of solar PV that the power system can accommodate while maintaining the voltage stability of the system. The literature [24] also applied the MOPSO technique to optimally size grid-connected ground mounted and rooftop PV system in Freetown, Sierra Leone, to reduce the daily generation cost and gap between generation and demand.

The importance of this research is thus three folds; it can help policy makers to understand the magnitude of Green House Gas (GHG) emissions obtained from thermal generation in Sierra Leone, though relatively small (under 0.03% of Global emissions) at the moment; it helps in providing both technical and economic basis for the adoption of suitable renewable energy technologies and the best hybrid options for integration; finally, it helps in establishing a holistic decision making process from resource availability to conversion and its environmental effects.

2. Methodology

An in-depth understanding of the extent of availability of renewable energy resources and the suitability in terms of the appropriate location to carryout the project is critical to establishing the financial viability of any of such projects. Fossil fuel technologies do not directly fall under this scope of assessment as the fuel resources are mostly located at or very close to the generating facilities. Policy makers thus need to be well informed about the quality, proximity of the resource to demand centers and take a closer look at the potential to reduce costs through the sharing of grid infrastructure and streamlined permitting [25]. At the moment there are limited comprehensive approaches that could be adopted for estimating national renewable energy generation in SSA. To help in overcoming this drawback, estimates of solar, wind, and biomass for every country in SSA has been done [26].

Amidst the several approaches adopted and mentioned in literatures [27,28], this study does not only focus on the technical and economic components of the factors that influence the viability of the project, but also throws light on the social and environmental sustainability of the project. Therefore, a summary indicating the inter dependency among the key components considered has been illustrated in the pentagonal relationship as highlighted in the bullets below and in Figure 1.

- **Political will**

  Usually in developing countries, public service providers and legal systems often lack the firmness and reliability over the medium to long term to institute and enforce policies governing private sector and supportive incentives for the integration of renewable energy. Therefore, the need for governments to give their political backing through the promulgation of energy policies with the necessary regulatory framework that would also encourage the private sector to invest in renewable energy systems for power delivery has become imminent [29]. The components of such policies include provision of long term investment security, drive upgrades of existing national grids and accelerate roll-out of mini-grids, address needs of non-electrical energy forms in productive sectors, energy efficiency improvement measures, and as much as possible, apart from operational and deployment activities, enhance domestic renewable energy technology manufacturing and assembly [30].

- **Resource assessment and suitability**

  The availability and suitability of any resource ensures that there is sufficient generating capacity to support the demand for targeted level of reliability with minimal cost. Hence carrying out critical assessment to determine the capacity factor of variable, uncertain and spatially diverse renewable energy resource using well-known methods, such as the Weibull distribution for wind assessment [31], is key to establishing the project viability. Data collection and identification of potential constraints that includes assessing of climatic factors, biographical factors, and geographical features such as altitude, temperature, densed urban areas, protected areas, large water bodies, etc. are also essential components in determining the suitability of the project [32].

- **Social and environmental sustainability assessment**

  This aspect involves the identification of mitigation measures that will not affect the livelihood of the project area negatively; keeping renewable harvest rates within regeneration rates; keeping

emissions to a bare minimum; ensuring that sources of raw materials needed by humanity should not be exhausted for electricity generation especially with regards biomass and hydro power generation; ensuring job creation [33]; and ensuring that livelihood of the inhabitants of the project area is improved.

- **Technology assessment**

  Renewable Energy Technologies (RETs) exist in a wide range of options for electricity generation; wind power generation can either be onshore or offshore; solar energy has solar heating, Concentrated Solar Power (CSP) and PV; hydro power has reservoir and run-of-the-river; and biomass power has combustion plants, biogas technology, grate technology, Bubbling Fluidized Bed (BFB) and Circulating Fluidized Bed (CFB), etc. This implies that selection of the preferred technology based on the resources available requires careful considerations ranging from type, fuel flexibility, load ramping capability, investment cost, and plant size [34] and thus the adoption of Clean Energy Technology Assessment Methodology (CETAM) [35].

- **Economic assessment**

  Many tools designed to allow policy makers to assess Cost Of Energy (COE) and Levelised Cost Of Energy (LCOE), cost-based incentive rates can be employed across global, regional, local, and project bases; National Renewable Energy Laboratory (NREL) models for economic evaluation of energy systems can be adopted; System Advisor Model (SAM); Cost of Renewable Energy Spreadsheet Tool (CREST), Job and Economic Development Impact (JEDI) Model, etc. [36].

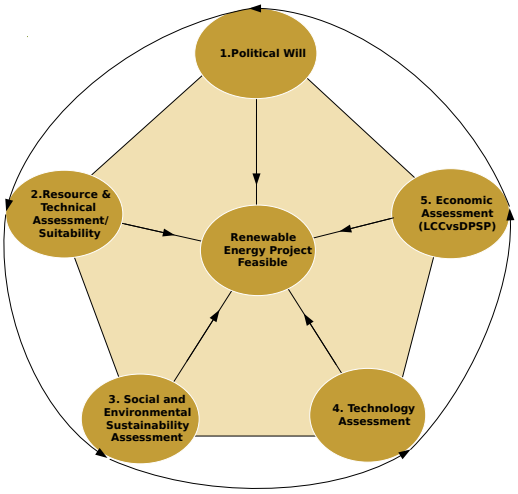

Figure 1. Pentagonal decision criteria for renewable energy integration.

2.1. Study Area

The scope of this research is nationwide. Table 1 lists all the existing generating facilities across the nation. However, not all generating facilities are in full operation due to aging and persistent operational problems. Hence their availability is very low and cannot be fully relied upon. Figure 2 shows the capacity of the existing RETs in the country for a period of 11 years to account for the slow development of RETs in the country. At the moment there is no grid connected PV and wind energy systems. The off grid PV installations mainly constitute solar street lights in selected parts of the country and few mini grids within the range of 6–36 kW. There is also no off-grid installation of wind turbines. Of the 15% electricity access, about 80% is dedicated to supply the capital city, Freetown, located in the Western area. This implies that for the remaining Eastern, Northern, and Southern regions where the bulk of the population resides, access to electricity is practically non-existent.

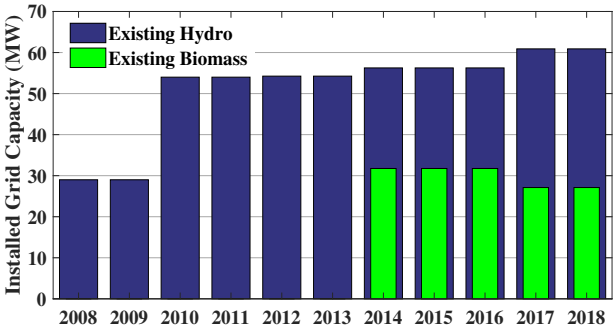

Figure 2. Existing renewable energy technologies.

Table 1. Existing generation facilities.

No.	Source	Capacity (MW)	Location
	Existing Sources		
1	Bumbuna Hydro	50	Bumbuna
2	Goma Hydro	6	Kenema
3	Charlotte Hydro	2	Western Area
4	Bankasoka Hydro	2	Port Loko
5	Diesel (Goverment)	27.6	Western Area
6	Diesel (Goverment)	26.7	Provincial
7	Diesel (IPP1)	20	Western Area
8	Diesel (IPP3)	4.8	Provincial
9	Addax Bio-energy	15	Makeni(Low availability)
10	**Total Diesel**	**139.1**	
11	**Total Hydro**	**60**	
12	**Total Biomass**	**15**	
13	**Total Generation**	**154.1**	
	Projected National Mining Power Demand[MW] (Approximated)		
1	Sierra Rutile	23(15)	Moyamba
2	Octea mining	8	Kono
3	London Mining	50	Marampa
4	Stella Diamonds	3	Tongo
5	African minerals/Shandong Iron and steel group	20 (150 PhaseII)	Tonkolili
6	Gold Mining and Others	20	Various locations
7	**Total Expected Generation**	**296**	
	Research Scope [MW]		
2	Approximated Industrial Demand	380	
3	Approximated Commercial Demand	150	
4	Approximated Domestic Demand	120	

These regions also host the major mining companies, as shown in Table 1, which rely entirely on captive generation to meet their energy requirements since the continuity and quality of energy supply are crucial to their energy requirements. Less than 2% of these companies are directly connected to the existing grid. Figure 3 shows the wide gap existing between generation and demand taking into consideration the utilization of existing energy generation, the operations and production patterns of industries using captive generation and their proposed expansions [37,38]. Since the existing grids do not cover the entire country, the accuracy of the profile is limited to ±25%.

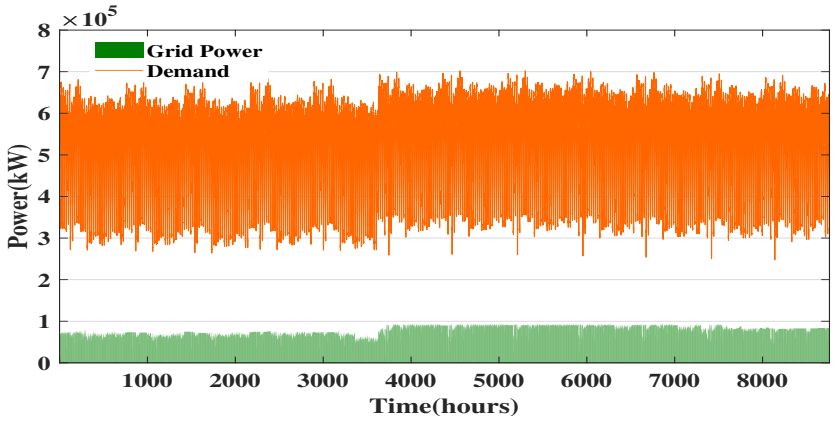

Figure 3. Grid power and demand.

The existing transmission and distribution infrastructure is one of the major constraints to expanding electricity access covering only about 40% of the residents in the Western area [39]. Hence, the industrial and commercial sectors have to greatly depend on running expensive diesel generators, giving rise to over 35,000 off-grid diesel generators. It is against this background that the government has partnered with donor organizations to urgently address the energy needs of the country. One of such partnerships have therefore caused the approval of the Coted'Ivoire, Liberia, Sierra Leone, and Guinea (CLSG) electricity networks interconnection project funded by the African Development Bank (AfDB), which involves the construction of a 1357 km long double high voltage (225 kV) line to connect the national networks of the four countries. The construction of this line is part of the priority projects of the West African Power Pool (WAPP) master plan [40,41] and completion of the construction work will bring about a huge boost in the generation sector as their will be enough transport capacity to cater for the energy needs of the country. The transmission line, as shown in Figure 4, almost evenly divides the entire country into halves, traversing seven districts. Hence in the subsections following, careful resource assessments have been done for wind, solar, and biomass along the proposed and existing grids in an attempt to preparing informed database for policy makers to access in their decision making.

2.2. Resource Assessment

Central to the development of variable renewable energy technologies, among other considerations such as demand, the nature of the network and required energy storage, a holistic planning process involves provision of an understanding of where the resources are strongest in order to enable reliability, increased generation, reduction of life cycle costs, helping policy makers develop policy incentives for renewable energy sources with the strongest potential, and, by extension, enable regional energy planners to appropriately reflect renewable energy contributions in their energy master plans [42]. Hence in this research well known methods have been used to make an approximate assessment of solar and wind energy potential and characteristics.

2.2.1. Wind Resource Assessment

Making accurate assessments of wind energy potential and characteristics requires long term meteorological observations [43]. For this study, one year analysis has been carried out on two locations; Kabala District in the Nothern region and Kenema District in Southern Region, denoted for simplicity as (**D1**) and (**D2**) respectively, along the proposed 225 kV as shown in Figure 4. Figure 5a,b shows the wind speed distribution for the two locations at 100 m hub height. Deployment of the renewable energy technology closer to the proposed infrastructure, denoted as (**B**) in Figure 4, will greatly reduce overall grid connection costs. Point (**C**) in the figure, denotes the proposed distance (within 30 km) from the existing and proposed grids to install the technologies. Among the many methods known

for wind assessment, Rayleigh and Weibull distributions have been widely used to describe the wind speed distribution [44,45]. The literature [44] also highlighted on the versatility of the 2-parameter Weibull distribution method and referenced the work of many researchers that have used it for wind profile characterization of any site. Hence, in this study, we have employed this method to carry out sensitivity analysis to determine the (***c***) and (***k***) values of the sites (**D1**) and (**D2**).

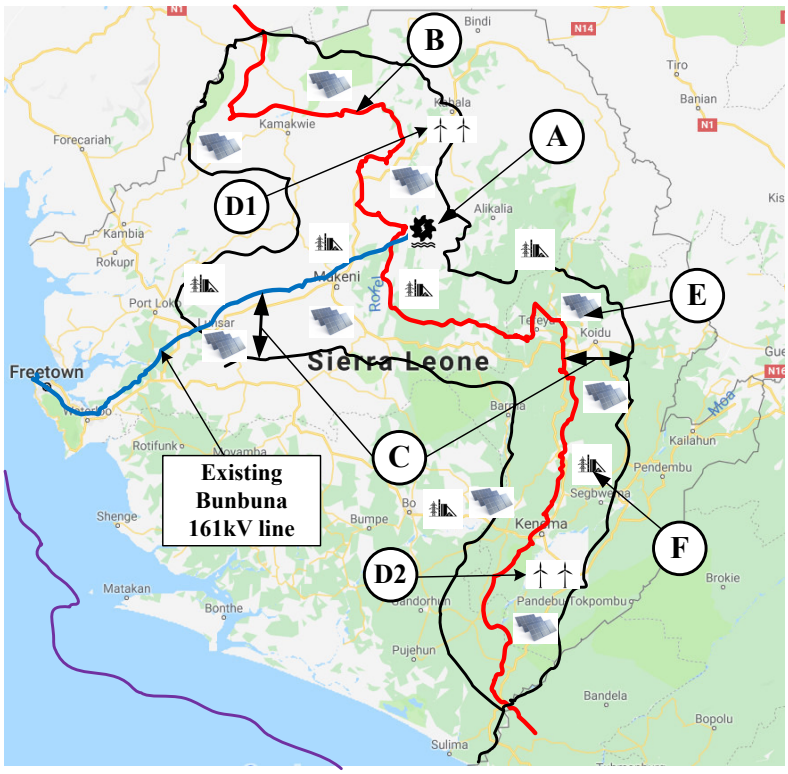

Figure 4. Photo-Voltaic (PV), biomass, and onshore wind centralized power plants suitability.

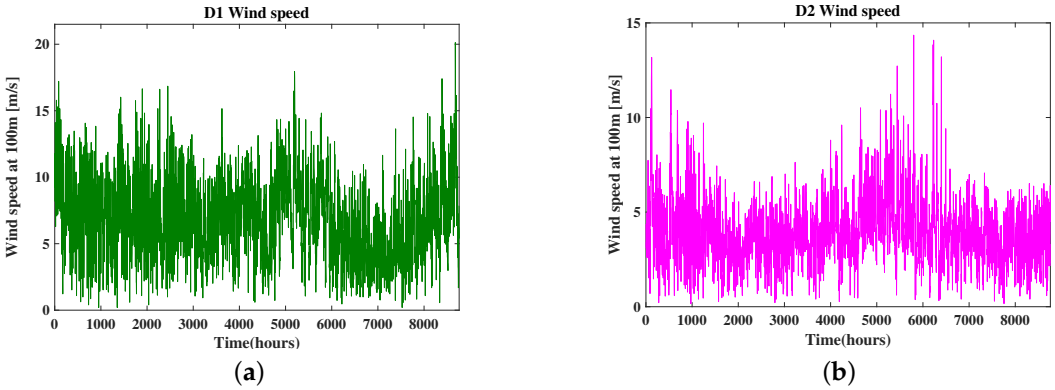

Figure 5. Assessment of wind farm locations. (**a**) D1 wind speed in the Northern region. (**b**) D2 wind speed in the Southern region.

The Weibull distribution function or Probability Density Function (PDF) is expressed mathematically as:

$$f(v) = \frac{k}{c}\left(\frac{v}{c}\right)^{k-1} exp\left[-\left(\frac{v}{c}\right)^{k}\right] \quad (1)$$

where *f(v)* is the probability of occurence of the observed wind speed v, k is the unitless Weibull shape parameter and c is the Weibull scale parameter.

The Cumulative distribution function (CDF) of the Weibull distribution is given by

$$f(v) = 1 - exp\left[-\left(\frac{v}{c}\right)^k\right] \tag{2}$$

where v, c, and k are the same as expressed in Equation (1). The maximum wind speed v_{max} and maximum frequency of the wind speed v_{mod} are expressed as:

$$v_{max} = c\left(\frac{k+2}{k}\right)^{\frac{1}{k}} \tag{3}$$

$$v_{mod} = c\left(1 - \frac{1}{k}\right)^{\frac{1}{k}} \tag{4}$$

Usually, wind power is expressed as:

$$P = \frac{1}{2}\rho A v^3 \tag{5}$$

where ρ (kg/m^3) is the air density taken to be 1.225 kg/m^3, A (m^2) is swept area. The Weibull wind power density PD, per unit area is given as:

$$p(v) = \frac{P(v)}{A} = \frac{1}{2}\rho c^3 \gamma\left(1 + \frac{3}{k}\right) \tag{6}$$

where γ is a gamma function. Since wind direction is much useful for positioning of wind turbines at the site, the assessment in this study is limited only to wind speed. Table 2 shows the scale and shape parameters and Power Density (PD) values for the sites. The scale parameter, c, indicates the intensity of the wind in the locations, whilst the shape parameter, k, indicates how peaked the wind distribution is [46].

Table 2. Weibull parameters and capacity factor.

Weibull Distribution Parameters				
Location	***c***	***k***	**PD (W/m^2)**	**CF**
D1	7.70	2.61	531.45	31.6
D2	4.75	2.40	189.40	9.95

Figure 6a–c shows the mean daily wind speed, PDF, and CDF for both locations. Figure 6d shows a simple model that simulates the electrical output power of the wind turbine generator. V_{ci}, V_r, and V_{co} are the cut-in, rated, and cut-off speeds, respectively, where the cut-in speed is necessary to start generating energy, the rated speed being the maximum yield point of the output power and the cut-off speed is the speed at which the generator stops in order to protect its mechanism. The behaviour of this system is usually expressed mathematically as shown in Equations (7) and (8) [44,47].

$$P_w(t) = \begin{cases} P_r \frac{V(t)^k - V_{ci}^k}{V_r^k - V_{ci}^k} & V_{ci} \le v(t) \le V_r \\ P_r & V_r \le v(t) \le V_{co} \\ 0 & v(t) > V_{co}, v(t) < V_{ci} \end{cases} \tag{7}$$

The average output power, $P_{w,avg}$, of the wind turbine is modeled as:

$$P_{w,avg} = P_r\left[\frac{e^{-\left(\frac{v_{ci}}{c}\right)^k} - e^{-\left(\frac{v_r}{c}\right)^k}}{\left(\frac{v_r}{c}\right)^k - \left(\frac{v_{ci}}{c}\right)^k} - e^{\left(\frac{v_{co}}{c}\right)^k}\right] \tag{8}$$

The capacity factor, CF, is expressed as:

$$CF_w = \frac{P_{w,avg}}{P_r} \quad (9)$$

The CF values for both locations have been listed in Table 2. These values are a measure of the energy production efficiency of that facility over a period of time based on the solar resource potential of the site. According to NREL's new transparent cost data base [48], of the 35 projects evaluated, onshore wind has a minimum capacity factor of 26%, a median value of 38%, and a maximum value of 52%. Therefore, from the values obtained, it is clearly seen that D1 location in the Northern province is preferred for wind farm installation as the capacity factor is relatively higher than that of D2 and above the minimum value of 26%. It shows that wind energy generation is possible especially in mountainous regions in the Northern part of Sierra Leone albeit, this value is obtained at 100 m hub height.

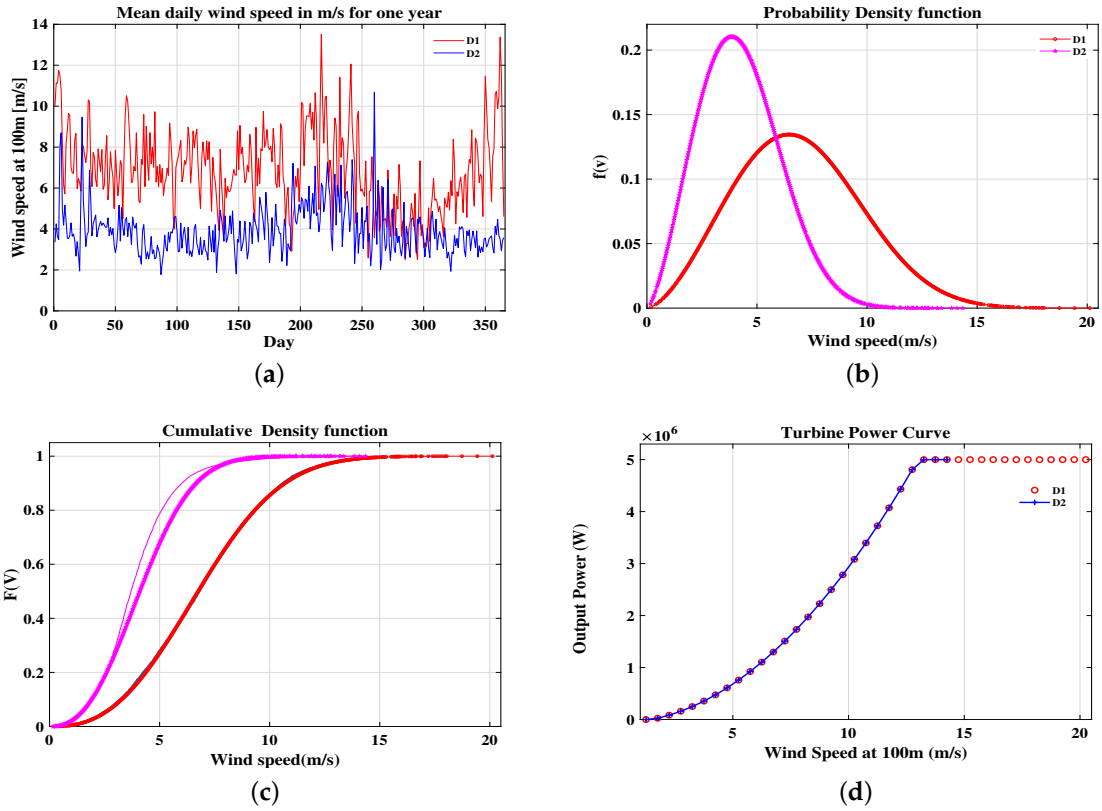

Figure 6. Assessment of wind farm locations continued. (**a**) Mean daily wind speeds of both locations. (**b**) Weibull probability density function. (**c**) Cumulative probability density function. (**d**) Turbine power curve for both locations.

2.2.2. Solar Resource Assessment

In the same manner for wind resource assessment, obtaining solar resource information is critical in the design stages of a solar project. Figure 7 shows the global horizontal irradiation (GHI) and suitability areas identified along the existing and proposed grids. Figure 8a,b shows the D1 and D2 solar radiations respectively. Analysis of monthly and annual values of GHI was carried out by the authors in [49,50]. For this research, we first obtained the CFs for both sites and were recorded as 27.41% and 25.13% for D1 and D2, respectively. The daily irradiation data for the best and worst days were then analysed to obtain the mean hourly distribution. The frequency count and probability distribution plots were obtained over a period of 1 year as shown in Figure 9a. The averaged hourly irradiance, G_t, is obtained from the Gaussian distribution function, $f(G_t)$, as expressed in Equation (12). From the statistical and probabilistic results obtained, it can be observed that the results for both sites

are closely marched. However, site D1 proves to be preferable since the CF obtained is slightly higher than the average CF for SSA (27%) [51]. Site D2 also shows good potential as the CF is higher than the mean value obtained for Solar projects at the NRELs new transparent cost data base (20.30%). Figure 9b shows the normalized PV generator power curve.

$$P_{pv}(t) = \begin{cases} P_{pvr}\left(\frac{G_t^2}{G_{std}R_c}\right) & \text{for } 0 \le G_t \le R_c \\ P_{pvr}\left(\frac{G_t}{G_{std}}\right) & \text{for } G_t > R_c. \end{cases} \quad (10)$$

$$CF_{pv} = \left\{ \frac{\sum_{t=1}^{8760} P_{pv}(t)}{8760 \times P_{pvr}} \right\} \quad \forall t, t \in T_y. \quad (11)$$

$P_{pv}(t)$ is the generated power at time t and P_{pvr} is the PV generator capacity assumed.

$$f(G_t) = \frac{1}{\sigma_{G_t}\sqrt{2\pi}} e^{-0.5\left(\frac{G_t - \mu_{G_t}}{\sigma_{G_t}}\right)^2} \quad (12)$$

where μ_{G_t} is the mean value and σ_{G_t} is the standard deviation of the solar radiation data set.

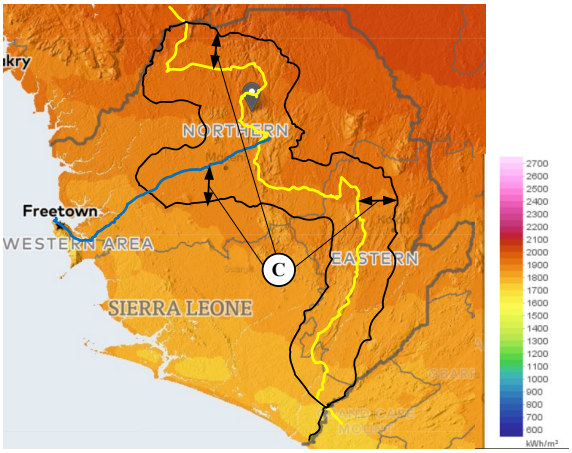

Figure 7. Global horizontal irradiation and PV suitability zone [52].

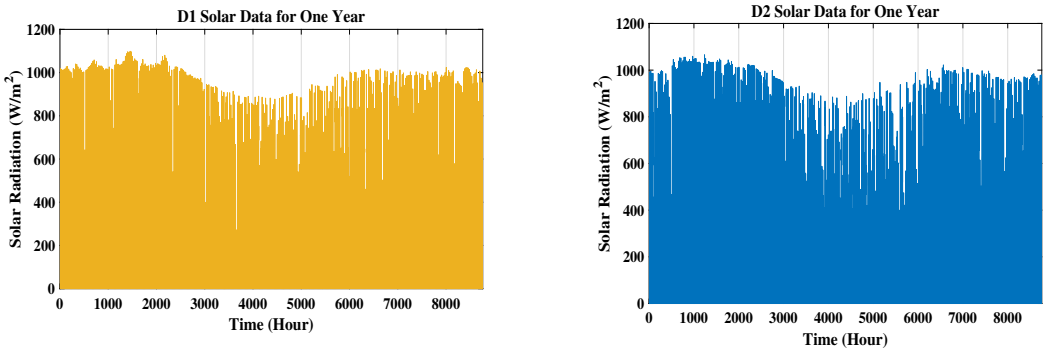

(**a**) (**b**)

Figure 8. Assessment of solar farm locations. (**a**) D1 solar irradiation in the Northern region. (**b**) D2 solar irradiation in the Southern region.

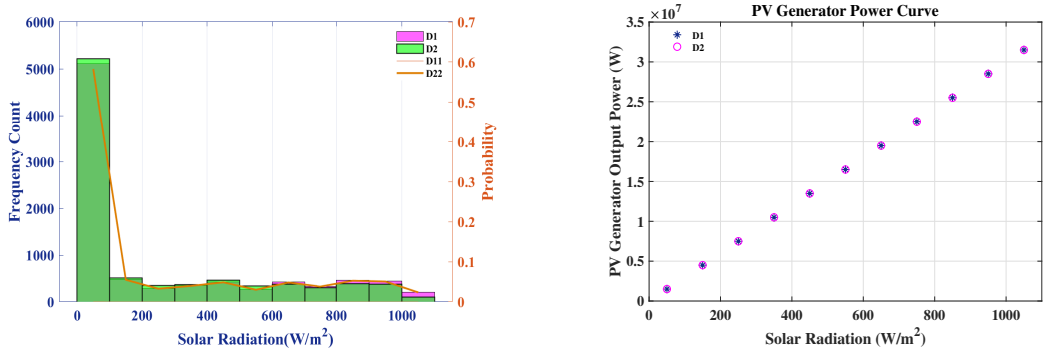

Figure 9. Assessment of solar farm locations.

2.2.3. Biomass Resource Assessment

There has been growing interest in the adoption of biomass in energy master plans worldwide mainly due to advances in biomass conversion technologies that bring out low GHG emissions. However, carrying out an assessment to map the location of the feedstock supply base with excess amount of land requiring least amount of resettlement, and quantify the minimum amounts of biomass needed is crucial to confirming the technical and financial feasibility of a biomass project in SSA. Determination of the security of supply, including supplier risks, seasonal variability, and the probable need for supplementary biomass feedstocks in the event of shortage of supply is all encompassing. The authors have highlighted several models for assessing biomass feedstock availability [34,53,54]. For this research, we focused on the assessment for the availability of sugarcane bagasse, a residue from sugarcane, to be used as fuel for the Circulating Fluidized Bed (CFB) biomass plant. Sugarcane bagasse has gained notoriety for use in eclectric power generation especially in Brazil, where its continuous usage to supply energy is increasing yearly [55]. Kambia district in Northern Sierra Leone has been considered the most suitable location for growing sugarcane because of its proximity to Freetown port (138 K) and Kolente river which provides access to irrigation [56]. Characterization of the biomass feedstock, which includes the physical and chemical properties, has been done in Table 3. Annual sugarcane production was obtained over 26 years as shown in Figure 10. The following calculation methodology was developed [34] to quantify the available sugarcane baggase, also known as supply potential, suitable for energy production annually:

$$Q_{Bagg} = S_{ann} \times K_{RB} \times K_{AC} \times K_{HC} \times K_{UF} \quad (13)$$

where Q_{Bagg} is the amount of sugarcane bagasse (tons) available for energy production, S_{ann} is the annual production of sugarcane(tons), K_{RB} is the ratio of sugarcane baggase to primary sugarcane (30%), K_{AC} is the accessibility coefficient (95%), K_{HC} is the harvest coefficient (100%), and K_{UF} is the unused fraction (80%) [34]. The current annual sugarcane production has been assumed to be the average production over the 26 years data obtained (70,000 tons/year). This implies that from Equation (13), the yearly supply potential of sugarcane bagasse is about 16,000 tons for energy production. Dedicated land would thus be required to increase the supply potential to 25,000 tons in order to meet the maximum desired capacity of the plant (45,000 kW). The selection of the appropriate biomass combustion power plant capacity is discussed in the Biomass System Model Section.

Table 3. Characterization of the biomass feedstock.

Biomass Feedstock Parameters				
Fuel Type	**NCV (MJ/kg)**	**Bulk Density (kg/m^3)**	**Ash Content (%Dry Bulk)**	**Moisture Content (%)**
Baggase briquette	16.7	650	6	8
Corncobs	14	185	15	14
Rice straw	14	100	20.25	10
Palm kernel shells	18.85	450	5	N/A

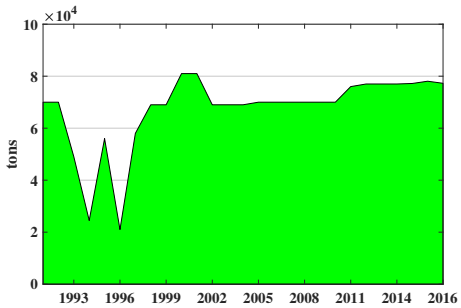

Figure 10. Annual sugarcane production [57].

3. Configuration and Scheme of Hybrid Systems

Ten combinations of hybrid systems have been introduced according to the scheme shown in Figure 11. The letters *A*, *B*, *C*, *D*, and *E* are used to designate the PV plant, wind turbines, biomass plant, battery bank, and diesel generator set, respectively, for ease of referencing the components of the blocks (Blocks 1–10) considered. The specifications of each component of the hybrid system for the respective blocks are fed into the optimization algorithm (MOPSO) as clearly illustrated in Figure 11. This process is explained in the next section (Problem Formulation). The configuration of the hybrid systems is representative of block 1 in Figure 12.

4. Problem Formulation

As seen in Figure 3, the gap between generation and demand is very wide and the grid power is dominated by diesel generation. In order to meet the electricity demand in the most economical and environmentally friendly manner, optimum configuration of wind, PV, biomass, DG, and BESS has been designed for 10 different hybrid blocks within certain levels of system reliability. The MOPSO algorithm is used to determine the optimal values of each block at a time. In addition to the brief highlight given in the Introduction Section, during the optimal operation each particle achieves the best fitness value and maintains that value. Then the particle with the best fitness value is calculated and updated during the iterative process. Each particle represents the configurations of the technologies to be considered (A, B, C, D, and E) for which the search space dimensions and the decision variables shown in Figure 11, will be 5. Each particle will then be evaluated by the multi-objective functions corresponding to LCC, DPSP, DEF, and CO_2 emissions. Hence in summary [58], the first step, which is the initialization involves requesting the input data of hourly radiation, wind speed, national demand requirements, all data to evaluate the technical and economic functions, and finally, data to access constraints for which upper and lower bounds have been stated in Equation (48). The energy output of the technologies are then calculated from Equations (14)–(21). Random selection of the position and velocity of particles is done to generate the initial population and applied to the objective functions for each iteration. The fitness value with minimum objective function is then calculated and updated. The updated value is then applied to find the optimal solution of the objective functions. If the objective functions for each combination is satisfied, then the optimal configuration for each combination is selected. Otherwise, the process starts again from evaluating and classifying the objective functions as shown in Figure 11. The optimality of the process is then confirmed after several runs of the

optimization process. The optimal values of DPSP (0%, 5%, 10%, 20%, 30%, 40%, and 50%) were deduced as indicators for policy makers to decide on the specific percentage of deficiency they want to achieve whilst carefully selecting which technologies would be appropriate to consider within the scope of the available resources. Therefore ten combinations were designed and evaluated whilst the LCC, DPSP, CO_2 emissions, and DEF were minimized. The LCC constitutes the capital cost (C_C), the Net Present Values (NPV) of the replacement cost (C_R), the resale cost (C_S), and the operations and maintenance costs (C_{OM}) of the technologies for each hybrid system.

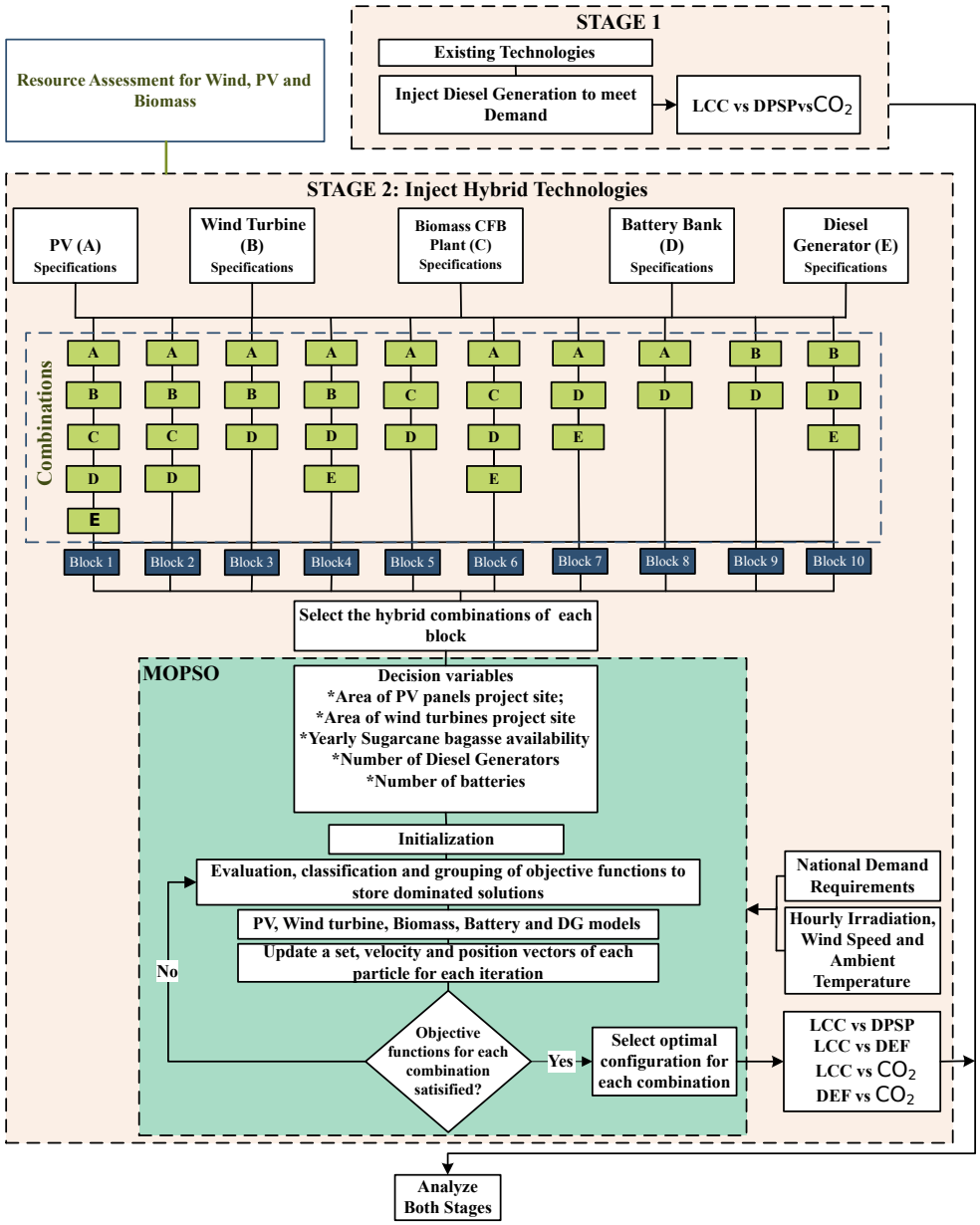

Figure 11. Scheme for hybrid energy systems injection.

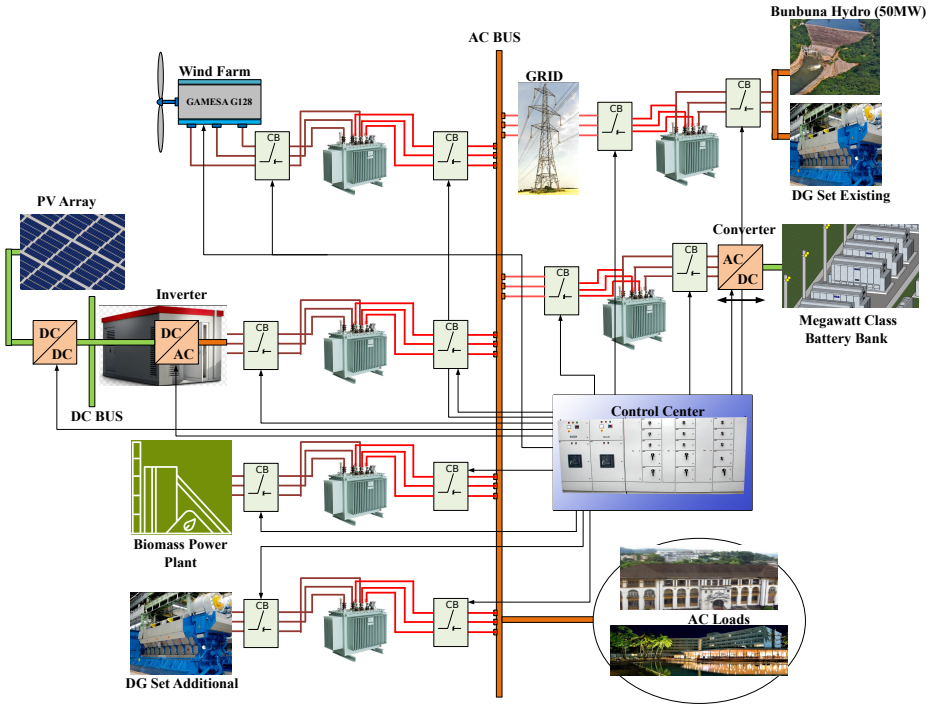

Figure 12. Configuration of hybrid system.

4.1. Physical System Criterion

For each of the combinations evaluated, the decision variables of the objective functions are land area occupied by PV panels (A_{PV}), area occupied by wind turbine's blades (A_W), quantity of baggase available for energy production (Q_{Bagg}), number of DG sets to be injected as additional back up power (Q_{DG}), and the battery bank capacity (Q_{Bat}). The performance of the PV panels and wind turbines depends on the meteorological conditions of the site. The amount of energy generated hourly by the systems is measured in kWh.

4.1.1. Wind System Model

The system behavior of the wind turbine is expressed mathematically as mentioned earlier in Equations (7) and (8). The decision variable is the total area swept by the wind turbine blades A_w and the rated power from Equation (7) is modelled as shown in Equation (14) below.

$$P_r = \frac{1}{2} \times C_p \times \rho_a \times \eta_w \times A_w \times V_r^3 \times 0.001 \quad (14)$$

where, ρ_a is the air density C_p is the power coefficient and η_w is the efficiency of the wind turbine. The rated power, P_r, is measured in kW. The adjustment of the wind profile from the reference hub height H_R (10 m), to the new hub height H (100 m), is given as [59]:

$$\frac{V_H}{V_{H_R}} = \left(\frac{H}{H_R}\right)^{\alpha} \quad (15)$$

V_H represent the wind speed (m/s) at 100 m hub height, V_{H_R} is the wind speed at 10 m hub height, and α is the roughness length index taken to be 0.14 for an area with low mature crops.

4.1.2. PV System Model

The decision variable for the PV system is the total area A_{pv} covered by the PV panels at the project site. The power supplied by the PV panels can be expressed as:

$$P_{pv} = G(t) \times \eta_{pv} \times A_{pv} \times 0.001 \quad (16)$$

where $G(t)$ is the hourly irradiation measured in watts per meter squared (W/m^2), η_{pv} is the efficiency of the PV module. P_{pv} is measured in kW.

4.1.3. Biomass System Model

For the CFB steam based power plant, the capacity per unit time was constrained to a maximum plant capacity of 45,000 kW, for which the maximum supply potential of baggase has been chosen to be 25,000 tons yearly. The dispatch scheme, illustrated in the reliability flow chart in Figure 13, is used to determine the yearly operating time T, of the plant. The decision variable, chosen to be the yearly supply potential of the plant Q_{Bagg}, is a function of this value T. An increase in the operating time would require a corresponding increase in Q_{Bagg} to maintain the desired output of the plant. This phenomenon is explained in the mathematical model expressed below [60]:

$$P_{BM} = \frac{0.278 \times Q_{Bagg} \times NCV_{Bagg} \times \eta_{CFB} \times 1000}{T} \quad (17)$$

where P_{BM} is the plant capacity (kW), Q_{Bagg} is determined from Equation (13) to be obtained from the optimization, NCV_{Bagg} is the net calorific value of baggase, η_{CFB} is the efficiency of the biomass plant, and T is the total yearly operating time. The CFB combustion plant was selected because it can be used in the mid range of 10–40 MWe and its excellent emission performance. Additionally, its fuel handling flexibility for feedstocks with low alkali content and typical moisture content values less than 60% [61] gives it advantage for this research scope over stoker grate boilers, which also uses baggase as one of its fuels.

4.1.4. DG System Model

A minimum plant unit, N_{DG} (10,000 kW), was selected for the diesel generator to be injected. The decision variable for this system is the total number of DG units, Q_{DG}, to be obtained from the optimization. The total generated output power of the DG is then formulated as:

$$P_{DES} = Q_{DG} \times N_{DG} \quad (18)$$

4.1.5. BESS Model

The battery energy storage is sized to meet the demand during periods of unavailability in accordance with the hybrid systems reliability flow chart. We have chosen the lithium ion battery bank for this research because of its high-cycle efficiency and fast response times. Recent advances in the technology development has rendered it cost competitive with that of the traditional lead acid battery. Additionally, lithium-ion represented more than 80% of the installed power and energy capacity of large-scale battery storage in operation in the United States at the end of 2016 in comparison with Lead acid, which represent 2%–3%, even though it is one of the oldest forms of battery storage [62]. The charging of the battery bank, represented by the state of charge (SOC) at any hour t, is calculated as follows:

$$SOC(t) = (SOC\,(t-1) \times (1-\delta_h)) + (P_{Gen}(t) - P_L(t)/\eta_I) \times \eta_{bc} \quad (19)$$

where $P_{Gen}(t) = P_{grid}(t) + P_{PV}(t) + P_W(t)$. The battery bank discharge at any time is given by:

$$SOC(t) = (SOC\,(t-1) \times (1-\delta_h)) - (P_{Gen}(t) + P_{BM}(t) + P_{DES}(t)) \times \eta_{bd} \quad (20)$$

The SOC at any given time is subject to the following constraint:

$$SOC_{min} \leq SOC(t) \leq SOC_{max} \quad (21)$$

where the minimum SOC is a function of the depth of discharge DOD, and nominal capacity of the battery bank C_B, given by $SOC_{min} = (1 - DOD) \times C_B$ with the DOD taken to be 50%.

4.2. Economic System Criterion

Evaluating the economic criterion for a project is key in optimizing the size of a hybrid energy system. For this research we have considered the project life N of all blocks evaluated to be 20 years. All economic parameters have been listed in Table A2. As mentioned earlier, the cost component considered is LCC. The constituent components were then evaluated in the next sections.

4.2.1. Wind System Model

Considering an initial cost of installation of one turbine to be α_w ($/m^2), the capital cost of investment is expressed as:

$$C_W = \alpha_w \times A_w \tag{22}$$

The lifespan of a wind turbine is considered to be 20 years. Therefore the replacement cost is zero ($R_{NPV_w} = 0$).

The annual operation and maintenance (OM_w) cost is expressed as: $\alpha_{OM_w} \times A_w$ ($/m^2/year). Since the annual growth rate of the cost is considered as μ_w and the interest rate is taken to be i, the NPV of the total O&M cost is given as:

$$OM_{NPV_w} = \alpha_{OM_w} \times A_w \times \sum_{j=1}^{N} \left(\frac{1+\mu_w}{1+i}\right)^j \tag{23}$$

The resale price is expressed as s_w ($/m^2). The total cost recovered from resale is given as $S_{w_{Tot}} = s_w \times A_w$. Hence, the resale price at the end of the project life is given as:

$$S_{NPV_w} = S_{w_{Tot}} \times \left(\frac{1+\delta_w}{1+i}\right)^N \tag{24}$$

The LCC of the wind power system is obtained as follows:

$$LCC_w = (C_W + OM_{NPV_w} + R_{NPV_w}) - S_{NPV_w} \tag{25}$$

4.2.2. PV System Model

Since the lifespan of the PV system is the same as the project life, the cost analysis follows the same procedure done for the wind system in Equations (22)–(25), whilst replacing the subscript w with the subscript pv.

4.2.3. Biomass System Model

As mentioned earlier, the decision variable for the biomass model is the quantity of baggase, Q_{Bagg} (tons). The total cost of supplying the baggase at the plant site is expressed as:

$$C_{Bagg_{Tot}} = (C_{baggase} + C_{storage} + C_{loading} + C_{transport}) \times Q_{Bagg} \tag{26}$$

where $C_{baggase}$, $C_{storage}$, and $C_{loading}$ are the cost of baggase, storage, and loading per ton of baggase respectively. $C_{transport}$ is the cost per ton of baggase per kilometer [34]. The capital cost of investment of the biomass plant is given as:

$$C_{BM} = \alpha_{BM} \times max(P_{BM}) \tag{27}$$

where $max(P_{BM})$ (kW) is the maximum output power of the biomass plant obtained from the optimization. The annual operation and maintenance cost, OM_{BM}, is expressed as: ($\alpha_{OM_{BM}} \times$

$sum(P_{BM})) + C_{Bagg_{Tot}}$ (\$/kWh/year). With the annual growth rate of the cost considered to be μ_{BM}, the NPV of the total O&M cost is given as:

$$OM_{NPV_{BM}} = OM_{BM} \times \sum_{j=1}^{N} \left(\frac{1+\mu_{BM}}{1+i}\right)^{j} \tag{28}$$

If the resale price is considered as s_{bm} (\$/kW), then the total cost recovered from resale is given as $S_{BM_{Tot}} = s_{bm} \times max(P_{BM})$. Hence, the resale price at the end of the project life is given by:

$$S_{NPV_{BM}} = S_{BM_{Tot}} \times \left(\frac{1+\delta_{BM}}{1+i}\right)^{N} \tag{29}$$

The replacement cost, $R_{NPV_{BM}}$, is considered to be zero. Therefore the LCC of the biomass power plant is obtained as follows:

$$LCC_{BM} = (C_{BM} + OM_{NPV_{BM}} + R_{NPV_{BM}}) - S_{NPV_{BM}} \tag{30}$$

4.2.4. DG System Model

For the cost analysis of the DG system considered to operate in dispatch mode as backup power, we employed the unit cost of \$1000/kW for 10,000 kW oil fired diesel plant. This cost was an approximate value obtained from cost estimates done for engines with nominal capacities of 40, 50, 100, and 160 MWe [63]. The choice of model for this study can be dual fuel MAN Engine, Nigatta, or Wartsila thermal engines that the workforce already has operational experiences with. The capital cost of the DG power plant, C_{DG}, to be installed for this scope of work is thus:

$$C_{DG} = \alpha_{DG} \times Q_{DG} \tag{31}$$

Since the DG plant is a dual fuel system, fuel consumption and cost analysis was done for Heavy Fuel Oil (HFO) and Diesel Oil (DO) operation based on the total yearly running hours, n, obtained from the optimization constrained by the dispatch schedule illustrated in Figure 13. The total fuel cost is therefore denoted as τ_{DG}. The annual O&M cost, (OM_{DG}), is given as $\alpha_{OM_{DG}} + \tau_{DG}$. The replacement cost is zero ($R_{NPV_{DG}} = 0$). Therefore, for a project life of 20 years, the total O&M ($OM_{NPV_{DG}}$) and resale ($S_{NPV_{DG}}$) costs are given by:

$$OM_{NPV_{DG}} = Q_{DG} \times OM_{DG} \times \sum_{j=1}^{N} \left(\frac{1+\mu_{DG}}{1+i}\right)^{j} \tag{32}$$

$$S_{NPV_{DG}} = S_{DG_{Tot}} \times \left(\frac{1+\delta_{DG}}{1+i}\right)^{N} \tag{33}$$

The LCC of the DG power plant is thus obtained as follows:

$$LCC_{DG} = (C_{DG} + OM_{NPV_{DG}} + R_{NPV_{DG}}) - S_{NPV_{DG}} \tag{34}$$

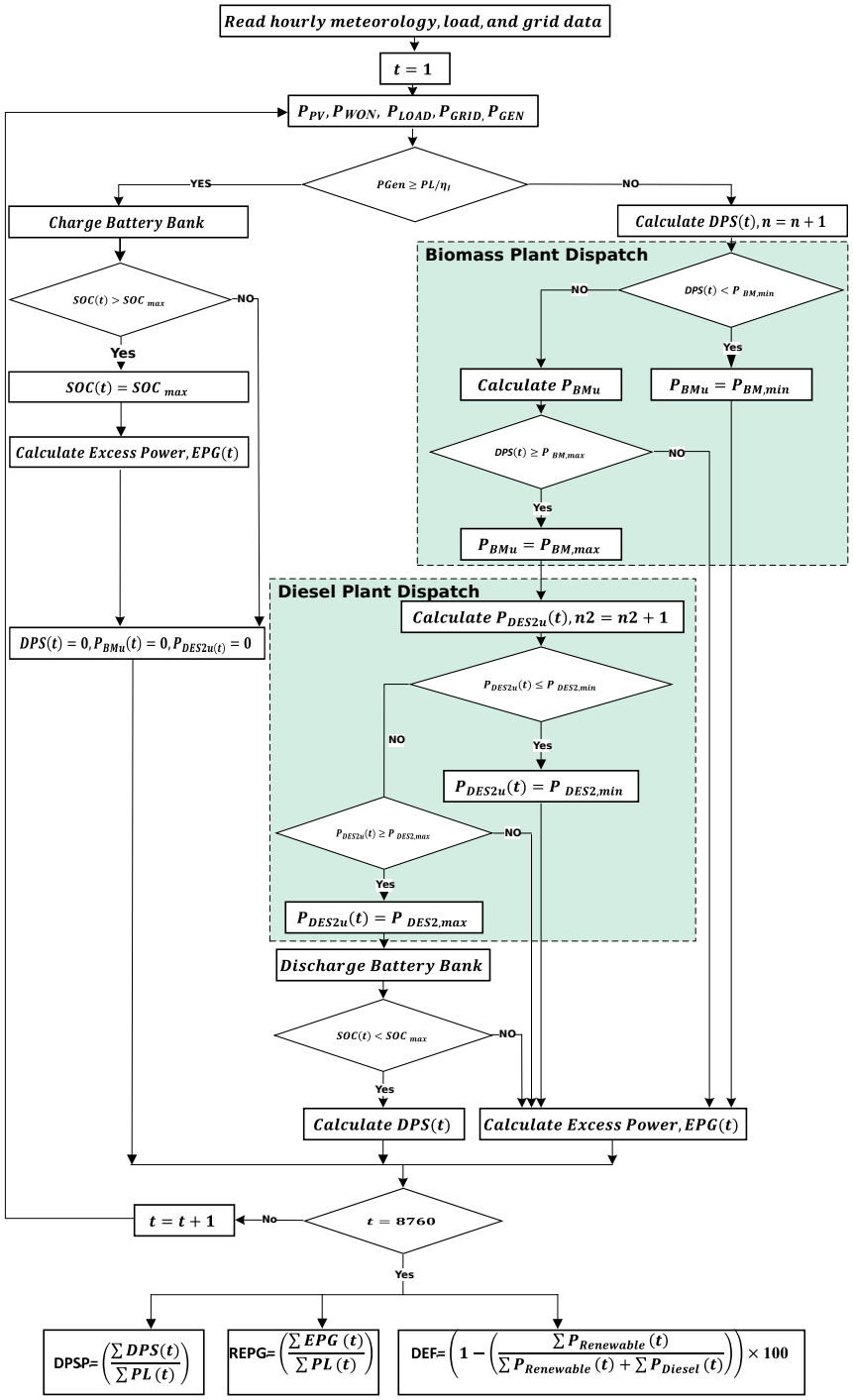

Figure 13. Reliability flow chart.

4.2.5. BESS System Model

The lifetime of the lithium ion battery bank is taken to be 10 years. The resale cost is zero ($S_{NPV_{Bat}} = 0$) and the capital cost of investment is given by:

$$C_{Bat} = \alpha_{Bat} \times Q_{Bat} \times C_b \tag{35}$$

where C_b is the nominal capacity of the battery bank. Since the project life is 20 years, the battery bank will be replaced once. Therefore the replacement cost after 10 years is expressed as:

$$R_{NPV_{Bat}} = C_{Bat} \times \left(\frac{1+\delta_{Bat}}{1+i}\right)^{j} \tag{36}$$

In this case, $j = 10$. The LCC of the BESS is therefore given by:

$$LCC_{Bat} = (C_{Bat} + OM_{NPV_{Bat}} + R_{NPV_{Bat}}) - S_{NPV_{Bat}} \tag{37}$$

4.3. Environmental Criterion

In this study, we have considered the Diesel Energy Fraction (DEF) and CO_2 emissions as the environmental performance indicators for each block. The DEF is the fraction of energy supplied from diesel generation. This fraction can be reduced by increasing the share of renewable energy and limiting the diesel operation to backup mode. The CO_2 emissions are therefore taken to be a function of the quantity of fuel burnt annually, Q_F, from the existing and injected diesel generation (HFO and DO) and the amount of baggase burnt from biomass generation. CO_2 emissions have been evaluated firstly, for 100% injection of diesel generation at certain levels of reliability from 0% to 50% and then compared against the hybrid blocks for the same levels of reliability as indicated in the case study and discussion of results section. Table A2 of Appendix A shows the Net Calorific Value (NCV) and Emissions Factors (EF_s) for HFO, DO, and Baggase. The CO_2 emissions coefficient, EF_s, of the fuel type, i, has been estimated in accordance with the default values given in the IPCC guidelines [64,65]. The fuel consumption for the existing dual fuel (HFO and DO) and light fuel oil (DO) engine models, as well as the injected engine model, have been listed in Table A1. Therefore, the DEF and amount of CO_2 emissions (Q_{CO_2}) produced yearly for all blocks have been expressed as:

$$DEF = \left(1 - \left(\frac{\sum P_{Renewable(t)}}{\sum P_{Renewable(t)} + \sum P_{DES(t)}}\right)\right) \times 100 \tag{38}$$

$$Q_{CO_2} = Q_{F,i} \times WEF_{F,i} \tag{39}$$

where $P_{Renewable(t)}$ is the total renewable generation, $P_{Diesel(t)}$ is the total generation from DG_s, $Q_{F,i}$ is the quantity of the ith fuel (HFO, DO, and Baggase) burnt annually, and $WEF_{F,i}$ is the weighted average emission factors of the ith fuel. $WEF_{F,i}$ is calculated as

$$WEF_{F,i} = NCV_i \times EF_{CO_{2,i}} \tag{40}$$

NCV_i is the weighted average net calorific value (mmBtu/gal) of the ith fuel and $EF_{CO_{2,i}}$ is the weighted average CO_2 emissions factor ($KgCO_2/mmBtu$) of the ith fuel. The annual CO_2 emissions avoided ($Ann_{CO_2,Avoided}$) by each block is determined from the difference between the reference emission (R_{emss}) and the block emissions (B_{emss}), as shown in the equation below:

$$Ann_{CO_2,Avoided} = R_{emss} - B_{emss} \tag{41}$$

This value gives policy makers a broad overview of the environmental friendliness of each combination as discussed in Section 5. The reference emission is the annual additional CO_2 emissions by the base case (DG Only) and the block emissions are the annual additional emissions caused by the injection of each block.

4.4. Hybrid Systems Reliability Criterion

We have used the DPSP to define the reliability of the system whilst biomass and DG plants are operated in dispatch mode, with priority given to biomass injection when PV and wind generation

cannot meet the load demand. The DPSP approach is considered as a technical criterion for sizing a hybrid system that employs a battery bank [66]. Figure 13 (reliability flow chart) illustrates the reliability model with the operational sequence summarized below:

- If the generated power, P_{Gen}, from the injected renewables (PV and Wind) is greater than the load demand, P_L, for a given time (t), the excess power is used to charge the battery bank as shown in Equation (19), until the $SOC(t) = SOC_{max}$. The new excess power, EPG, is unused.
- If P_L is greater than the energy generated from PV and wind injection, the deficiency of power, DPS, is calculated and biomass power, P_{BM}, is used to meet the deficit until the maximum intended capacity of P_{BM} is obtained. If the deficit is less than the intended minimum injection of biomass $P_{BM_{min}}$, then the capacity of P_{BM} is taken to be $P_{BM_{min}}$. However, if the deficit is greater than the intended maximum biomass power, P_{BM}, then the capacity of biomass power is taken to be $P_{BM_{max}}$. The new deficit is calculated and diesel generation, P_{DES}, is used to meet the deficit. The minimum and maximum diesel generation, $P_{DES_{min}}$ and $P_{DES_{max}}$, respectively, are used to constrain the diesel generation in the same manner as described for the biomass injection.
- When the calculated $P_{DES} \geq P_{DES_{max}}$, this implies there is still deficit. In this case the battery bank is discharged according to Equation (20) to satisfy the demand. If the $SOC(t) < SOC_{max}$ the new deficit, $DPS(t)$, is calculated. Otherwise, $EPG(t)$ is calculated. The excess and deficient power for any given hour, t, are thus expressed as follows:

$$EPG(t) = P_{Gen}(t) - [P_L(t)/\eta_I + (P_{BM}(t) + P_{DES}(t) + (SOC_{max} - SOC(t-1))/\eta_{bc}))] \quad (42)$$

$$DPS(t) = P_L(t)/\eta_I - (P_{Gen}(t) + P_{BM}(t) + P_{DES}(t)) \quad (43)$$

where $P_{Gen}(t) = P_{grid}(t) + P_{PV}(t) + P_W(t)$. For this research we have calculated the EPG to determine the unused power generated by the system. The Relative Excess Power (REPG) and DPSP are evaluated as shown in the reliability flow chart. Values of DPSP obtained from the optimization that are equal to or closer to 0 implies the load will be always or nearly satisfied. Hence, policy makers can have an insight into the cost and environmental implications simultaneously, when choosing any block for a desired DPSP.

4.5. Summary of Objectives

The objective functions considered for this study are thus summarized below:

$$OF_{ECO} = min\,(LCC_W + LCC_{PV} + LCC_{BM} + LCC_{DG} + LCC_{BAT}) \quad (44)$$

$$OF_{DEF} = min\left\{\sum_{t=1}^{8760}(DEF(t))\right\} \quad (45)$$

$$OF_{DPSP} = min\left\{\sum_{t=1}^{8760}\left(\frac{\sum DPS(t)}{\sum PL(t)}\right)\right\} \quad (46)$$

$$OF_{ENV} = min\left\{\sum_{t=1}^{8760}[Q_{F,i} \times WEF_i]\right\} \quad (47)$$

where OF_{ECO}, OF_{DEF}, OF_{DPSP}, and OF_{ENV} are the economic objective or LCC, DEF, DPSP, and environmental objective or CO_2 emissions respectively.

5. Case Study and Discussion of Results

The technical, environmental, and economic parameters of the PV system, wind farm, biomass plant, DG plant, and battery bank applied in the different hybrid blocks considered are listed in Table A2 of Appendix A. Upper bounds were established on the decision variables based on resource availability and suitability. Therefore, the total area swept by the wind turbines' blades, PV panel

project area, quantity of baggase available for energy production, number of DG units, and the battery bank capacity have been varied accordingly below:

$$\begin{bmatrix} 1.0e3 \leq A_{PV} \leq 6.0e6 \\ 1.3e4 \leq A_W \leq 9.0e6 \\ 1.0e3 \leq Q_{Bagg} \leq 2.5e4 \\ 1 \leq Q_{DG} \leq 30 \\ 10 \leq Q_{Bat} \leq 800 \end{bmatrix} \quad (48)$$

The total project areas allocated for PV system and Wind farm installations occupies less than 0.03% of the total land area of Sierra Leone (71,740 km^2), thereby posing no threat to the living area of the inhabitants.

Two-parameter Weibull distribution and Gaussian distribution methods were used to assess the potential of wind and PV where the capacity factors revealed that wind generation is feasible in Kabala (Site D1) with a capacity factor of 31.6% for 100 m hub height as compared to capacity factor of 9.95% in Kenema (Site D2). Capacity factors of 27.41% and 25.13% also revealed the feasibility of PV injection at sites D1 and D2, respectively. Biomass resource assessment revealed that in order to achieve a maximum injection of 45 MW additional 9000 tons of yearly baggase supply is needed to complement the 16,000 tons of baggase obtained. This would require a dedicated land at or near the plant site as mentioned in the Section 2.2.3. Multi-objective optimization technique using MOPSO was applied to follow the reliability model with the objective of minimizing DPSP, DEF, LCC, and CO_2 emissions. In order to justify the accuracy of the considered algorithm, several runs were made for each block from which the best solutions were deduced. The optimal results were evaluated and compared for different values of DPSP (0–50%). It was observed that due to maintaining the upper bounds of the resources consistently across all blocks, DPSP values ranging from 0–50% were obtained for 5 blocks whilst DPSP values from 30–50% were obtained for the remaining 5 blocks. In order to avoid ambiguity in the analysis, comparison on blocks with DPSP values within the range of 0–50% has been done in Tables 4 and 5. Figure 14 shows the optimal pareto front plots obtained within this range, whilst Figure A1 in Appendix A shows plots for the remaining blocks that has DPSP values in the range 30–50% respectively.

5.1. Annual Avoided CO_2 Emissions on Varying Reliability Options for Each Combination

The annual avoided CO_2 emissions for each block have been evaluated against the set of DPSP values as shown in Table 4 and Figure 15. Figure 16 illustrates the actual emissions intensity for the various levels of reliability. DG only block has been considered as base case for comparing the performance of the other blocks. From the results obtained it can be observed that blocks 3 (ABD), 8 (AD), and 9 (BD) are the most environmentally friendly since they have the highest avoided emissions for all levels of DPSP. High levels of CO_2 emissions are realized in the base case scenario (DG Only) due to the daily operation of DGs to meet demand. Figures 15 and 16 clearly shows that Block 1 (ABCDE) has moderately low emission values as compared to blocks 7 (ADE) and the base case. This is clearly seen in the amount of tCO_2 emissions avoided yearly by Block 1 for each DPSP level. This shows that increasing the share of renewable technologies with DG operated only in backup mode can considerably reduce CO_2 emissions. Block 7 is seen to be pretty high for 10% and 20% DPSP. However, in order to reach a conclusion on the choice blocks appropriate for the level of reliability that could be decided by policy makers, LCC values were evaluated as well in the next subsection.

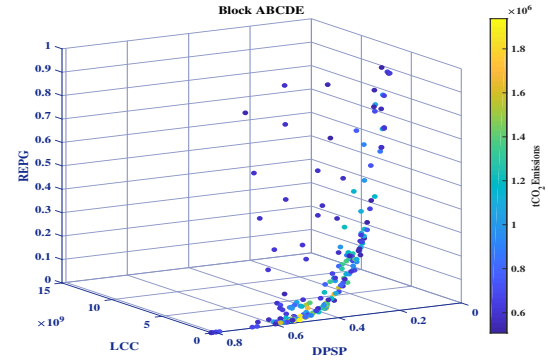

(**a**)

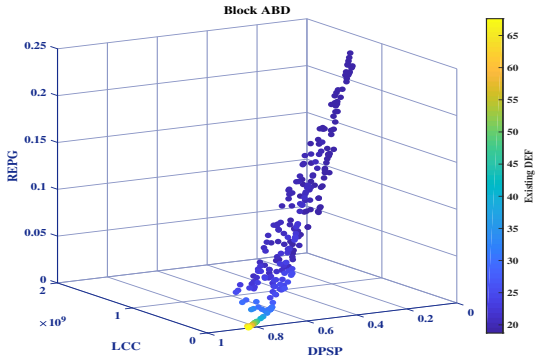

(**b**)

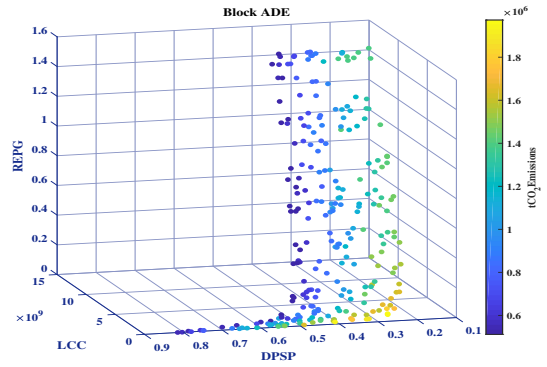

(**c**)

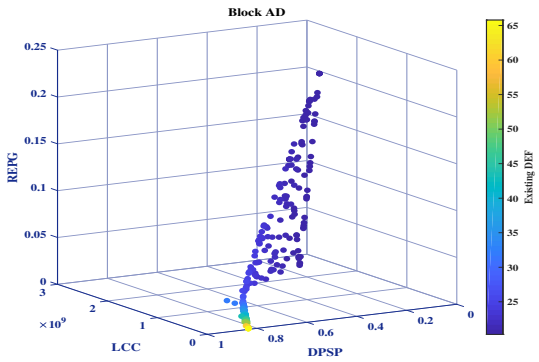

(**d**)

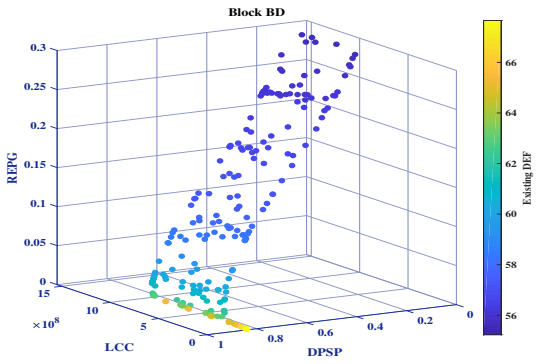

(**e**)

Figure 14. Pareto front plots for blocks with DPSP values within 0–50%.

Table 4. Annual avoided CO_2 emissions for each block.

BLOCK	Parameter	DPSP						
		0%	**5%**	**10%**	**20%**	**30%**	**40%**	**50%**
DG Only	*Annual Additional CO_2 Emissions*	1.75×10^6	1.64×10^6	1.53×10^6	1.33×10^6	1.11×10^6	9.15×10^5	7.21×10^5
B1-ABCDE	*Annual CO_2 Avoided Emissions* (tCO_2)	1.75×10^6	1.48×10^6	1.34×10^6	8.66×10^5	7.46×10^5	4.90×10^5	5.80×10^5
B3-ABD		1.75×10^6	1.64×10^6	1.53×10^6	1.33×10^6	1.11×10^6	9.15×10^5	7.21×10^5
B7-ADE		1.75×10^6	1.64×10^6	5.76×10^5	4.67×10^5	6.73×10^5	7.47×10^5	6.70×10^5
B8-AD		1.75×10^6	1.64×10^6	1.53×10^6	1.33×10^6	1.11×10^6	9.15×10^5	7.21×10^5
B9-BD		1.75×10^6	1.64×10^6	1.53×10^6	1.33×10^6	1.11×10^6	9.15×10^5	7.21×10^5

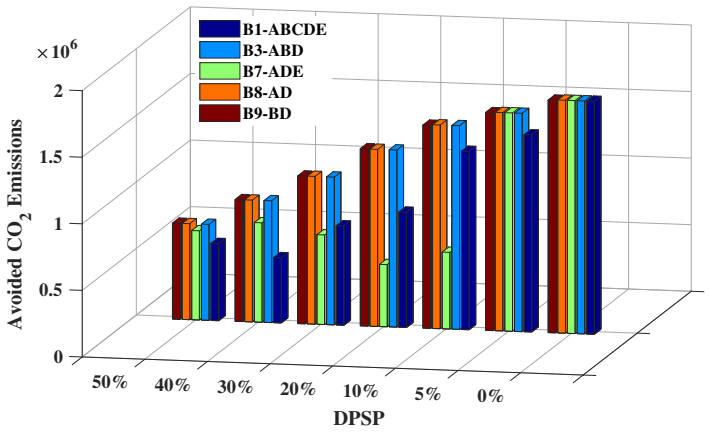

Figure 15. Annual avoided CO_2 emissions by each block.

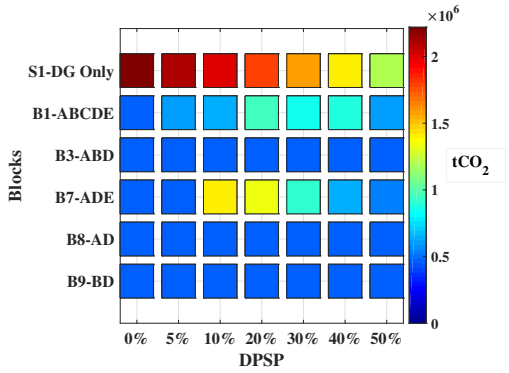

Figure 16. Actual CO_2 emissions intensity.

5.2. LCC Outcomes on Varying Reliability Options for Each Combination

LCC values were compared for the base case and the blocks considered in this literature in order to determine the most economical grid scenario. Table 5 and Figures 17 and 18 fully describe this scenario. The capital costs of the technologies and on-site capacity factors for the wind and solar PV obtained earlier from the assessments conducted significantly influence the LCC values for each block. Usually, technologies with lower investment costs and higher on-site capacity factors result in lower LCC. We observed that the base case is the most expensive grid scenario due to the significantly high penetration of DGs running for a longer term as seen from the high DEF values, high capital costs, and operations and maintenance costs. For example, considering a 90% electricity access (DPSP of 10%), running DGs only would cost the government an LCC of 6.14 Bn USD over 20 years. Block 1 (ABCDE) was also observed to have comparatively high LCC value for DPSP of 5% (2.23 Bn USD). This outcome resulted from high penetration of low capacity factor solar PVs (27.41%) for the site selected and biomass plant with high capital investment and total operations cost. However, as seen from Table 5 and Figure 17, block 1 has the lowest LCC values from 20% (1.0 Bn USD) to 50% (380 M USD) DPSP for the project life of 20 years, which makes it very competitive with the other blocks. Block 9 (BD) has the lowest LCC values for 0%, 5%, and 10% DPSP. Block 3 (ABD) also has lower LCC values than block 9 for reliability levels of 40% and 50%.

Table 5. Comparison of selected blocks from the results obtained.

Block	Parameter	DPSP						
		0%	**5%**	**10%**	**20%**	**30%**	**40%**	**50%**
DG Only	Q_{DG}	63	59	55	48	40	33	26
	DEF	95	94.4	94	93.3	92.4	91	89.3
	LCC	7.02×10^9	6.58×10^9	6.14×10^9	5.35×10^9	4.47×10^9	3.68×10^9	2.89×10^9
B1-ABCDE	A_{PV}	-	2.2×10^6	1.5×10^6	6.1×10^5	1.7×10^5	1.3×10^5	2.9×10^4
	A_W	-	1.3×10^6	8.1×10^5	7.4×10^5	6.0×10^5	2.6×10^5	4.3×10^5
	Q_{Bagg}	-	2.5×10^4	1.7×10^4	4.5×10^3	4.5×10^9	4.5×10^9	7.3×10^9
	Q_{DG}	-	14.0	12.5	19.6	13.0	13.0	1.0
	Q_{Bat}	-	35	54.7	56.5	10	10	97.2
	DEF	-	7.2	13.2	37.2	37.7	55.2	22.5
	REPG	-	0.44	0.25	0.12	0.06	0.00	0.02
	LCC	-	2.23×10^9	1.52×10^9	1.0×10^9	6.2×10^8	3.9×10^8	3.8×10^8
B3-ABD	A_{PV}	1.5×10^6	1.5×10^6	1.4×10^6	1.5×10^6	1.5×10^6	7.2×10^5	3.9×10^5
	A_W	9.0×10^5	8.8×10^5	8.7×10^5	8.2×10^5	7.7×10^5	8.4×10^5	8.4×10^5
	Q_{Bat}	372.13	280.1778	118.0276	126.0121	174.812	90.516	181.9352
	DEF	18.7	18.9	19.2	19.6	20.1	22.2	23.8
	REPG	0.14	0.14	0.15	0.11	0.06	0.04	0.01
	LCC	1.6×10^9	1.5×10^9	1.4×10^9	1.4×10^9	1.4×10^9	9.7×10^8	8.4×10^8
B7-ADE	A_{PV}	-	-	5.8×10^6	5.6×10^6	5.35×10^6	5.0×10^6	14.5×10^6
	Q_{DG}	-	-	35	24	11	4	1
	Q_{Bat}	-	-	130	128	125	120	120
	DEF	-	-	19.8124	21.2465	15.0873	20.9012	19.5347
	REPG	-	-	0.86	0.66	0.77	0.14	0.10
	LCC	-	-	3.57×10^9	3.303×10^9	3.12×10^9	2.94×10^9	2.61×10^9
B8-AD	A_{PV}	4.0×10^6	3.9×10^6	3.8×10^6	3.7×10^6	3.4×10^6	3.2×10^6	3.0×10^6
	Q_{Bat}	773.8	577	470.8	523.2	430.8	319.5	156.3
	DEF	19.6	19.8	20.2	20.9	21.7	23.0	23.9
	REPG	0.01	0.06	0.07	0.01	0.00	0.01	0.01
	LCC	2.8×10^9	2.6×10^9	2.5×10^9	2.4×10^9	2.3×10^9	2.0×10^9	1.8×10^9
B9-BD	A_W	1.3×10^6	1.3×10^6	1.2×10^6	1.2×10^6	1.1×10^6	1.1×10^6	1.0×10^6
	Q_{Bat}	840	799.3	765.7	737.8	541.8	410	548.5
	DEF	55.4	55.2	55.7	56.1	56.5	56.8	57.3
	REPG	0.32	0.36	0.28	0.22	0.18	0.16	0.11
	LCC	1.43×10^9	1.41×10^9	1.3×10^9	1.3×10^9	1.1×10^9	9.8×10^8	1.1×10^9

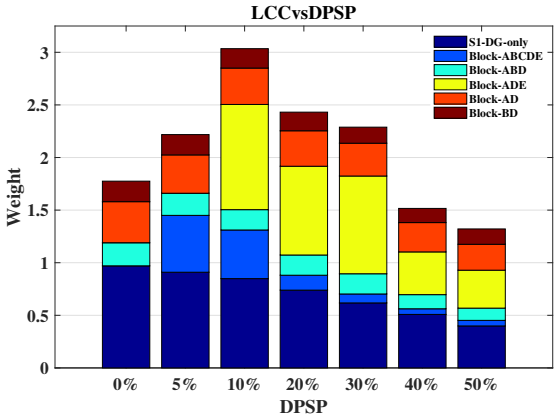

Figure 17. Life Cylce Cost (LCC) values evaluated against Defficiency of Power Supply Probability (DPSP).

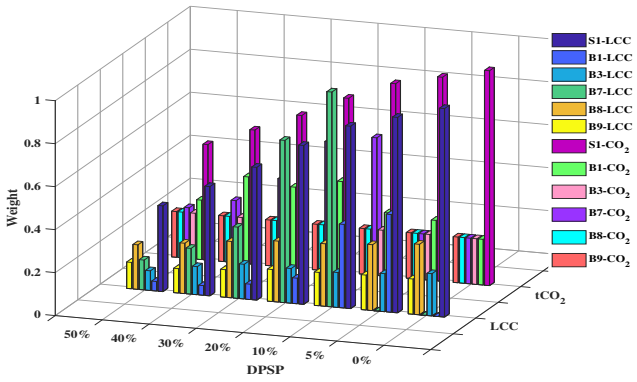

Figure 18. Weighted LCC and CO_2 emissions for each block.

6. Conclusions

A multi-criteria decision maker for grid-connected renewable energy systems in Sierra Leone was considered as the Sub-Saharan African case. A pentagonal relationship was used to summarize the inter dependency of the key components that should be considered to determine the feasibility of any renewable energy project. A fair resource assessment of solar PV, wind, and biomass power potential was done for the district towns of Kabala, Kenema, and Kambia, where the PV plant, wind farm, and biomass plant will be constructed to be connected along the proposed WAPP 225 kV line and closer to the existing grid. The results from the assessment revealed that Site D1 at Kabala district has the highest capacity factor for PV (27.41%) and Wind (31.6%), indicating that the Northern region is most feasible for installing solar PV panels and wind turbines. The biomass assessment also revealed the need for a dedicated land for an additional 9000 tons of yearly bagasse supply to achieve the maximum capacity of 45 MW. Ten hybrid combinations were studied in order to establish the most economical and environmentally friendly hybrid combinations for the selected technologies. The input data set for the MOPSO algorithm consists of hourly solar global irradiation, wind speed, load requirements for the year 2017, and specifications of the system devices. The optimum results revealed that Block 1, a combination of PV, wind, biomass, BESS, and DG, has low LCC values, 1.0 Bn USD to 380 M USD for a wider range of DPSP values of 20% to 50%, respectively. At 10% DPSP, Bolck 1 has an LCC value of 1.5 Bn USD, which is also very competitive with the LCC of the other blocks for the same level of reliability. The heat tiles (Figure 16 and Table 4) show moderately low CO_2 emissions for Block 1. From the perspective of job creation, the fraction of each renewable energy technology considered in the respective blocks influences the average employment gained in construction, installation, O&M and fuel processing jobs. This study, however, did not deal with the quantitative analysis of job creation due to limited data obtained. However, from the methodologies adopted by [67,68], considering a rich energy mix and creating jobs in the agricultural sector as well, block 1 is the most ideal for a wider scope of sectors, from Agriculture to Construction, for the locations considered. Therefore, we have recommended Block 1 to achieve the long term goals of the government, which is 92% electricity access (a DPSP of approximately 10%) by 2030, as mentioned in Section 1.

In our future work, we intend to include quantitative analysis to accurately determine the job creation potentials of each block for all the reliability levels, whilst evaluating the power trading potential within the Cote d'ivoire, Liberia, Sierra Leone, and Guinea block in the West African Power Pool. As we look forward to making more contributions we hope this information will add to the database of similar work to help policy makers in the region.

Author Contributions: The main idea, methodology, development of algorithms and data acquisition of this paper was proposed and obtained by D.A.K. All authors contributed to the data analysis, development of algorithm and writing of the final manuscript. All authors read and approved the final manuscript.

Acknowledgments: The authors acknowledge the unwavering support of the co-wokers of D.A Konneh, operations staff of the Electricity Generation and Transmission Company and the Distribution Supply Authority of Sierra Leone, for helping in providing relevant data with regards the daily operations of the power plants across the country.

Conflicts of Interest: The authors delcare no conflict of interests

Abbreviations

The following abbreviations are used in this manuscript:

k	unitless Weibull shape parameter.
c	Weibull scale parameter.
v	observed wind speed.
$f(v)$	probability of occurrence.
v_{max}	maximum wind speed.
v_{mod}	maximum frequency of wind speed.
ρ_a	air density.
A	swept area.
γ	gamma function.
P_w	output power of wind tubine.
P_r	rated power of turbine.
V_{ci}	cut-in wind speed.
V_r	rated wind speed.
V_{CO}	cut-off wind speed.
$P_{w,avg}$	average output power of wind turbine.
CF_w	capacity factor.
P_{pv}	generated power from PV panel.
P_{pvr}	PV generator capacity.
G_t	solar radiation data set.
G_{std}	standard solar radiation (1000 W/m^2).
R_c	radiation threshold (180 W/m^2).
CF_{pv}	capacity factor of PV.
T_y	total number of hours in a year.
μ_{G_t}	mean value of the solar radiation data set.
σ_{G_t}	standard deviation of the solar radiation data set.
Q_{Bagg}	amount of sugarcane bagasse (tons) available for energy production.
S_{ann}	annual production of sugarcane.
K_{RB}	ratio of sugarcane baggase to primary sugarcane.
K_{AC}	accessibility coefficient.
K_{HC}	harvest coefficient.
K_{UF}	unused fraction.
C_p	power coefficient.
η_w	efficiency of the wind turbine.
A_w	total area swept by the wind turbine blades.
V_H	wind speed at 100 m hub height.
V_{H_R}	wind speed at 10 m height .
H_R	reference hub height (10 m).
α	roughness length index.
A_{pv}	the total area of PV system.
η_{pv}	efficiency of the PV module.
P_{BM}	plant capacity of biomass.
NCV_{Bagg}	net calorific value of baggase.
η_{CFB}	efficiency of the biomass plant.
T	yearly operating time.
P_{DES}	diesel generation.
Q_{DG}	total number of DG units.

N_{DG}	minimum plant unit of diesel generator.
$SOC(t)$	state of charge of battery.
δ_h	hourly self discharge
$P_L(t)$	load demand.
η_I	efficiency of inverter.
η_{bc}	battery charging efficiency.
η_{bd}	battery discharge efficiency.
SOC_{min}	minimum SOC.
SOC_{max}	maximum SOC.
DOD	depth of discharge.
α_w	initial cost of turbine.
C_W	captial cost of investment.
OM_{NPV_w}	net present value of annual operation and maintenance cost of wind turbine.
α_{OM_w}	operation and maintenance cost of wind tubine.
NPV	net present value
S_{NPV_w}	NPV of the resale price of wind turbine.
s_w	resale price.
$S_{w_{Tot}}$	total cost recovered from resale.
N	total yearly running hours.
LCC_w	LCC of wind power system.
R_{NPV_w}	NPV of the replacement cost of wind turbine.
$C_{Bagg_{Tot}}$	total cost of supplying the baggase at the plant site.
$C_{Baggase}$	cost of baggase.
$C_{storage}$	cost of storage.
$C_{loading}$	cost of loading.
$C_{transport}$	tansport cost.
C_{BM}	capital cost of investment of biomass plant.
α_{BM}	initial cost of biamass plant.
$OM_{NPV_{BM}}$	NPV of the total operation and maintenance cost.
μ_{BM}	annual growth rate of the BM cost.
μ_{BM}	annual growth rate of the BM cost.
OM_{BM}	annual operation and maintenance cost of BM.
$S_{NPV_{BM}}$	NPV of the resale price of biomass plant.
$S_{BM_{Tot}}$	total cost recovered from resale.
δ_{BM}	initial cost of biomass plant.
LCC_{BM}	life cylce cost of biomass power plant.
$OM_{NPV_{BM}}$	NPV of the total operation and maintenance cost of biomass plant.
$R_{NPV_{BM}}$	NPV of the replacement cost of biomass plant.
C_{DG}	capital cost of the DG power plant.
α_{DG}	initial cost of DG.
$OM_{NPV_{DG}}$	NPV of the total operation and maintenance cost of DG.
OM_{DG}	operation and maintenance cost of DG.
μ_{DG}	annual growth rate of the DG cost.
$S_{NPV_{DG}}$	NPV of the resale price of DG.
$S_{DG_{Tot}}$	total resale price of DG at the end of the project life.
δ_{DG}	initial cost of DG plant.
LCC_{DG}	life cylce cost of DG.
C_{DG}	capital cost of investment of DG.
$OM_{NPV_{DG}}$	NPV of the total operation and maintenance cost of DG.
$R_{NPV_{DG}}$	replacement cost of DG.
C_{Bat}	captial cost of battery system.
α_{Bat}	initial cost of battery system.
C_b	nominal capacity of battery.
$R_{NPV_{Bat}}$	replacement cost of battery.
δ_{Bat}	initial cost of battery.

LCC_{Bat}	life cylce cost of battery.
C_{Bat}	capital cost of investment of battery.
$OM_{NPV_{Bat}}$	NPV of the total operation and maintenance cost of battery.
$S_{NPV_{Bat}}$	NPV of the resale price of battery energy storage.
$P_{Renewable}$	the total renewable generation.
$Q_{F,i}$	quantity of the ith fuel burnt annually.
$WEF_{F,i}$	weighted average emission factor of the ith fuel.
NCV_i	weighted average net calorific value.
$EF_{CO_{2,i}}$	weighted average CO_2 emissions factor.
$Ann_{CO_2,Avoided}$	Avoided amount of CO_2 emission.
R_{emss}	reference emissions.
B_{emss}	block emissions.
EPG	new excess power.
P_{Gen}	generated electric power.
DPS	deficiency of power.
MOPSO	multi-objective particle swarm optimization.
DG	diesel generator.
DEF	diesel energy fraction.
DPSP	defficiency of power supply probability.
LCC	life cycle cost.
PV	photovoltaic.
RDG	renewable distributed generator.
GHG	green house gas emissions.
GA	genetic algorithm.
PSO	particle swarm optimization.
RET	renewable energy technology.
CFB	circulating fluidized bed.
WAPP	west african power pool.
AfDB	african development bank.
GHI	global horizontal irradiance.
SSA	sub-saharan africa.
HFO	heavy fuel oil.
DO	diesel oil.

Appendix A

Table A1 shows fuel consumption values for the existing DG units considered in this study and Figure A1 shows the pareto plots for blocks with DPSP values within the range of 30–50%. Table A2 lists all parameters used in this study.

Table A1. Fuel Consumption of DG units across the country.

Fuel Consumption for Existing DG units Considered			
DG unit	**Fuel Operation**	**Number of Units**	**Consumption (l/h)**
A	Diesel Oil	20	240
B1	Diesel Oil	3	350
B2	Diesel Oil	5	240
K	Heavy Fuel oil	2	700
	Diesel Oil		620
L	Heavy Fuel oil	3	470
	Diesel Oil		430
N1 and N2	Heavy Fuel oil	2	1024
	Diesel Oil		981

Table A1. *Cont.*

Fuel Consumption for Existing DG units Considered			
DG unit	**Fuel Operation**	**Number of Units**	**Consumption (l/h)**
W1 and W2	Heavy Fuel oil	2	1300
	Diesel Oil		1230
M	Diesel Oil	2	300
LO	Diesel Oil	1	300
MA	Diesel Oil	1	240

Table A2. Physical, Environmental, and Economic Parameters.

Physical and Environmental Parameters			
Technology Type	**Variable**	**Notation**	**Value**
Wind Turbine GAMESA G128-5.0 MW/G132-5.0 MW	Rated Power	P_r (kW)	5000
	Cut-in speed	V_c (m/s)	1.5
	Rated Speed	V_r (m/s)	13
	Cut-off speed	V_{co}	27
	HubHeight	H (m)	100
	Wind Turbine lifetime	L_W	20
PV Panel Sun Power X Series	Maximum Power	$P_{PV,max}$ (W)	360
	Efficiency of Panel	η_{PV}	22.2
	Area of PV panel	A_{PV_p} (m^2)	1.63
	PV lifetime	L_{PV}	20
Biomass CFB Combustion Plant	Net calorific value of Baggase	NCV_{Bagg} (MJ/Kg)	16
	Baggase Emissions Factor	$EF_{CO_2,Bagg}$ (mmBtu/kg)	0.0161
	Efficiency of Plant	η_{CFB}	0.42
	Lifetime of Biomass plant	L_{BM}	20
Diesel Generator (DG) Nigatta Dual Fuel Diesel Plant	Unit Plant Capacity	$N_{DG}(MW)$	10,000
	Lifetime of DG plant	L_{DG}	20
	Net calorific value of Heavy Fuel Oil (HFO)	NCV_{HFO} (mmBtu/gal)	0.15
	Net calorific value of Diesel Oil (DO)	NCV_{DO} (mmBtu/gal)	0.148
	HFO Emissions Factor	EF_{HFO,CO_2} ($kgCO_2$/mmBtu)	75.1
	DO Emissions Factor	EF_{DO,CO_2} ($kgCO_2$/mmBtu)	74.92
Battery Bank Lithium Ion	Hourly Self Discharge	δ	0
	Battery charging efficiency	η_{bc}	0.9
	Battery Discharging efficiency	η_{bd}	0.9
	Nominal Capacity of Battery (kWh)	C_B	1200
	Lifetime of Battery Bank	L_{Bat}	10
Economic Parameters			
	Project lifetime	N	20
	Interest rate	i (%)	10
	Inflation rate	δ (%)	4
	Escalation rate	μ (%)	5
	Inverter efficiency	η_I (%)	90
Wind Turbine	Capital cost of Wind Turbine	C_W ($/$m^2$)	544
	Yearly Operations and Maintenance Cost	α_{OM_w} ($\%ofC_W$)	1.5
	Reselling Price	s_w ($\%ofC_W$)	30
PV Panel	Capital cost of PV Panel	C_{PV} ($/kW)	519.7
	Yearly Operations and Maintenance Cost	$\alpha_{OM_{PV}}$ ($\%ofC_{PV}$)	1
	Reselling Price	s_{pv} ($\%ofC_{PV}$)	25
Biomass Plant	Capital cost of Biomass Plant	C_{BM} ($/kW)	1440
	Cost of Bagasse	$C_{baggase}$ ($/ton)	25
	Cost of Storage	$C_{storage}$ ($/ton)	12
	Cost of loading	$C_{loading}$ ($/ton)	5
	Cost of Transportation	$C_{transport}$ ($/ton/km)	0.057
	Yearly Operations and Maintenance Cost	$\alpha_{OM_{BM}}$ ($\%ofC_{BM}$)	0.017
	Reselling Price	s_{bm} ($\%ofC_{BM}$)	30
Diesel Generator	Capital cost of DG plant	C_{DG} ($/kW)	1000
	Cost of HFO	C_{HFO} ($/litre)	0.45
	Cost of DO	C_{DO} ($/litre)	0.607
	HFO Consumption	Q_{HFO} (litre/hour)	1024
	DO Consumption	Q_{DO} (litre/hour)	981
	Yearly Operations and Maintenance Cost	$\$\alpha_{OM_{DG}}$ ($/kWh)	0.032
	Reselling Price	s_{dg} ($\%ofC_{DG}$)	30
Battery Bank	Capital Cost of Battery	C_{DG} ($/kW)	283
	Replacement Cost	R_{Bat}	-

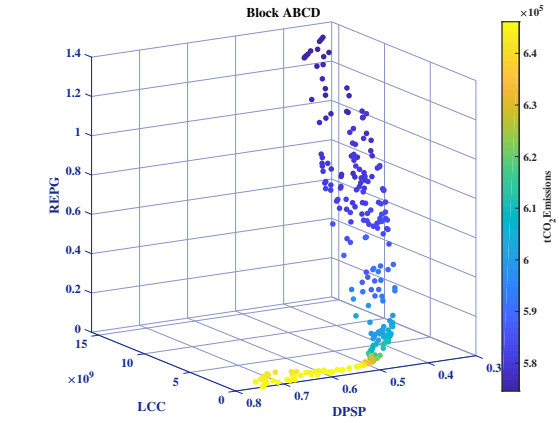

(**a**)

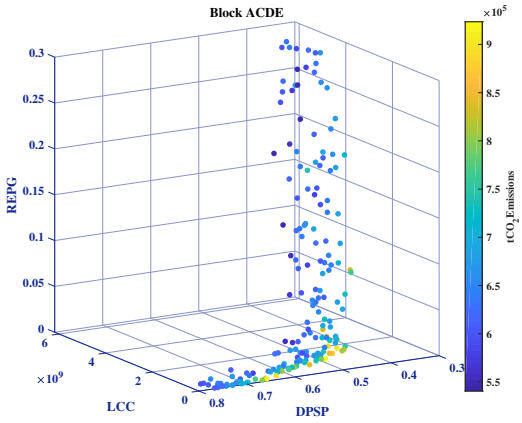

(**b**)

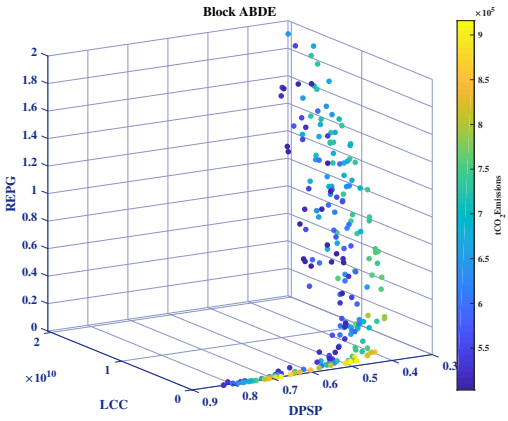

(**c**)

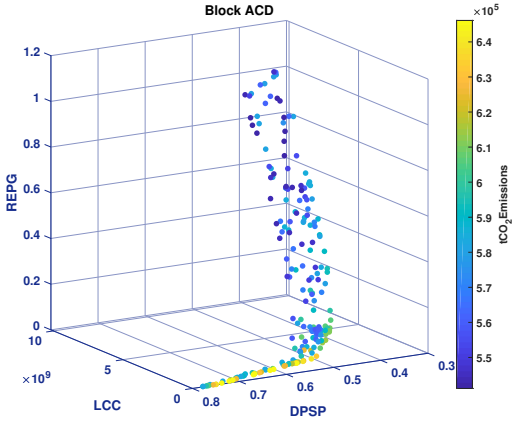

(**d**)

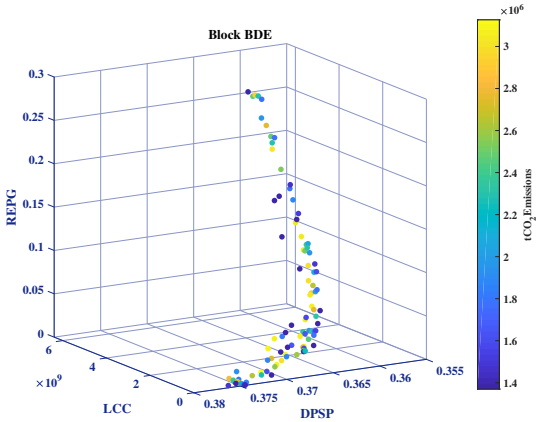

(**e**)

Figure A1. Pareto front plots for Blocks with DPSP values within 30–50%.

References

1. Lee, J.T.; Callaway, D.S. The cost of reliability in decentralized solar power systems in sub-Saharan Africa. *Nat. Energy* **2018**, *3*, 960–968. [CrossRef]
2. *Special Report: Energy Access Outlook*; International energy Agency: France, 2017. Available online: http://www.iea.org (accessed on 10 August 2018).
3. Sierra Leone Unemployment Rate. The Statistics Portal. Available online: https://www.statista.com (accessed on 30 August 2018).
4. Sierra Leone Sustainable Energy For All (SE4ALL) Country Action Agenda: Sustainable Energy For All. 30 July 2015. Available online: https://www.se4all-africa.org (accessed on 30 August 2018).
5. Tolba, M.; Rezk, H.; Tulsky, V.; Diab, A.; Abdelaziz, A.; Vanin, A. Impact of Optimum Allocation of Renewable Distributed Generations on Distribution Networks Based on Different Optimization Algorithms. *Energies* **2018**, *11*, 245. [CrossRef]
6. González, A.; Riba, J.R.; Rius, A. Optimal Sizing of a Hybrid Grid-Connected Photovoltaic–Wind–Biomass Power System. *Sustainability* **2015**, *7*, 12787–12806. [CrossRef]
7. Nižetić, S.; Papadopoulos, A.; Tina, G.; Rosa-Clot, M. Hybrid energy scenarios for residential applications based on the heat pump split air-conditioning units for operation in the Mediterranean climate conditions. *Energy Build.* **2017**, *140*, 110–120. [CrossRef]
8. Vishnupriyan, J.; Manoharan, P. Multi-criteria decision analysis for renewable energy integration: A southern India focus. *Renew. Energy* **2018**, *121*, 474–488. [CrossRef]
9. Theodorou, S.; Florides, G.; Tassou, S. The use of multiple criteria decision making methodologies for the promotion of RES through funding schemes in Cyprus, A review. *Energy Policy* **2010**, *38*, 7783–7792. [CrossRef]
10. Usman, M.; Khan, M.T.; Rana, A.S.; Ali, S. Techno-economic analysis of hybrid solar-diesel-grid connected power generation system. *J. Electr. Syst. Inf. Technol.* **2018**, *5*, 653–662. [CrossRef]
11. Saiprasad, N.; Kalam, A.; Zayegh, A. Techno-economic and environmental analysis of hybrid energy systems for a university in Australia. *Aust. J. Electr. Electron. Eng.* **2018**, *15*, 168–174. [CrossRef]
12. Alharthi, Y.Z.; Siddiki, M.K.; Chaudhry, G.M. Resource Assessment and echno-Economic Analysis of a Grid-Connected Solar PV-Wind Hybrid System for Different Locations in Saudi Arabia. *Sustainability* **2018**, *10*, 3690. [CrossRef]
13. Adaramola, M.; Oyewola, O.; Paul, S. Technical and Economic Assessment of Hybrid Energy Systems in South-West Nigeria. *Energy Explor. Exploit.* **2012**, *30*, 533–551. [CrossRef]
14. Barakat, S.; Samy, M.; Eteiba, M.; Wahba, W. Feasibility Study of Grid Connected PV-Biomass Integrated Energy System in Egypt. *Int. J. Emerg. Electr. Power Syst.* **2016**, *17*. [CrossRef]
15. Eichman, J.; Mueller, F.; Tarroja, B.; Smith Schell, L.; Samuelsen, S. Exploration of the integration of renewable resources into California's electric system using the Holistic Grid Resource Integration and Deployment (HiGRID) tool. *Energy* **2013**, *50*, 353–363. [CrossRef]
16. Yimen, N.; Hamandjoda, O.; Meva'a, L.; Ndzana, B.; Nganhou, J. Analyzing of a Photovoltaic/Wind/Biogas/Pumped-Hydro Off-Grid Hybrid System for Rural Electrification in Sub-Saharan Africa—Case Study of Djoundé in Northern Cameroon. *Energies* **2018**, *11*, 2644. [CrossRef]
17. Ou, T.C.; Hong, C.M. Dynamic operation and control of microgrid hybrid power systems. *Energy* **2014**, *66*, 314–323. [CrossRef]
18. Ismail, M.; Moghavvemi, M.; Mahlia, T. Genetic algorithm based optimization on modeling and design of hybrid renewable energy systems. *Energy Convers. Manag.* **2014**, *85*, 120–130. [CrossRef]
19. Robles Rodriguez, C.; Bideaux, C.; Guillouet, S.; Gorret, N.; Roux, G.; Molina-Jouve, C.; Aceves-Lara, C. Multi-objective particle swarm optimization (MOPSO) of lipid accumulation in Fed-batch cultures. In Proceedings of the 2016 24th Mediterranean Conference on Control and Automation (MED), Athens, Greece, 21–24 June 2016; pp. 979–984. [CrossRef]
20. Comparison of Three Evolutionary Algorithms: GA, PSO, adn DE. *Ind. Eng. Manag. Syst.* **2012**, *11*, 215–223. [CrossRef]
21. Ting Li, B.Y. A Review of Multi-objective Particle Swarm Optimization Algorithms in Power System Economic Dispatch. *Int. J. Simul. Syst. Sci. Technol.* **2016**, *17*, 1–5. [CrossRef]

22. Theo, W.L.; Lim, J.S.; Ho, W.S.; Hashim, H.; Lee, C.T. Review of distributed generation (DG) system planning and optimisation techniques: Comparison of numerical and mathematical modelling methods. *Renew. Sustain. Energy Rev.* **2017**, *67*, 531–573. [CrossRef]
23. Adewuyi, O.B.; Shigenobu, R.; Senjyu, T.; Lotfy, M.E.; Howlader, A.M. Multiobjective mix generation planning considering utility-scale solar PV system and voltage stability: Nigerian case study. *Electr. Power Syst. Res.* **2019**, *168*, 269–282. [CrossRef]
24. Konneh, D.A.; Lotfy, M.E.; Shigenobu, R.; Senjyu, T. Optimal Sizing of Grid-connected Renewable Energy System in Freetown Sierra Leone. *IFAC-PapersOnLine* **2018**, *51*, 191–196. [CrossRef]
25. Knight, O. *Assessing and Mapping Renewable Energy Resources*; World Bank, Washington, DC, USA. Available online: http://www.esmap.org (accessed on 15 September 2018).
26. Sebastian Hermann, Asami Miketa, N.F. *Estimating the Renewable Energy Potential in Africa*; International Renewable Energy Agency: Abu Dhabi, UAE, 2014. Available online: http://www.irena.org (accessed on 20 September 2018).
27. Løken, E. Use of multicriteria decision analysis methods for energy planning problems. *Renew. Sustain. Energy Rev.* **2007**, *11*, 1584–1595. [CrossRef]
28. Wang, J.J.; Jing, Y.Y.; Zhang, C.F.; Zhao, J.H. Review on multi-criteria decision analysis aid in sustainable energy decision-making. *Renew. Sustain. Energy Rev.* **2009**, *13*, 2263–2278. [CrossRef]
29. Remco Fischer, Jenny Lopez, S.S. Barriers and Drivers to Renewable Energy Investment in Sub-Saharan Africa. *J. Environ. Investig.* **2011**, *2*, 54–80.
30. A Framework for Transforming Africa towards a Renewable Energy Powered Future With Access for All. Africa Renewable Energy Initiative (AREI). 2015. Available online: https://www.arei.org (accessed on 10 October 2018).
31. Arslan, T.; Bulut, Y.M.; Altın Yavuz, A. Comparative study of numerical methods for determining Weibull parameters for wind energy potential. *Renew. Sustain. Energy Rev.* **2014**, *40*, 820–825. [CrossRef]
32. Lee, N.; Roberts, B. *Technical Potential Assessment for the Renewable Energy Zone (REZ) Process: A GIS-Based Approach*; National Renewable Energy Laboratory, United State Department of Energy, USA, 2018. Available online: https://www.nrel.gov/docs/fy18osti/71004.pdf (accessed on 15 October 2018).
33. Dorji, G. *Environmental Aspect of Electric Energy Generation*; Available online: https://www.researchgate.net/publication/296672956_Environmental_aspect_of_electric_energy_generation (accessed on 23 February 2019).
34. Glenting, C.; Jakobsen, N. *Converting Biomass to Energy: A Guide for Developers and Investors (English)*; World Bank Group: Washington, DC, USA, 2017. Available online: http://documents.worldbank.org (accessed on 20 October 2018)
35. Adam Brown, Simone Landolina, E.M.; Sung, J. *The Clean Energy Technology Assessment Methodology: International Energy Agency Laboratory*; OECD/IEA: Paris, France, 2016. Available online: https://www.iea.org (accessed on 25 October 2018).
36. Economic and Financial Analysis Tools: National Renewable Energy Laboratory. Available online: https://www.nrel.gov/analysis/economic-financial-tools.html (accessed on 25 October 2018).
37. BCS. Mining Industry Energy Bandwidth Study. 2007. Available online: https://www.energy.gov/eere/amo/downloads/us-mining-industry-energy-bandwidth-study (accessed on 27 October 2018).
38. Sierra Rutile Limited. Ruidow Conference 2016. 2016. Available online: https://sierrarutile.iluka.com/reports (accessed on 27 October 2018).
39. Project Appraisal Document. World Bank Group. Report No: 103305-SL. 2016. Available online: https://www.worldbank.org (accessed on 25 October 2018).
40. Ministry of Energy Progress Report. Government of Sierra Leone. 2017. Available online: https://www.energy.gov.sl/wp-content/uploads/.../ProgressReportMoE.pdf (accessed on 25 October 2018).
41. Asami Miketa (IRENA), Bruno Merven (Energy Research Center). West African Power Pool: Planning and Prospects for Renewable Energy. 2013. Available online: https://www.irena.org (accessed on 25 October 2018).
42. Estimating the Renewable Energy Potential in Africa: A GIS-Based Approach. 2014. Available online: https://www.irena.org (accessed on 31 October 2018).

43. Akdağ, S.A.; Dinler, A. A new method to estimate Weibull parameters for wind energy applications. *Energy Convers. Manag.* **2009**, *50*, 1761–1766. [CrossRef]
44. Ajayi, O.O.; Fagbenle, R.O.; Katende, J.; Ndambuki, J.M.; Omole, D.O.; Badejo, A.A. Wind Energy Study and Energy Cost of Wind Electricity Generation in Nigeria: Past and Recent Results and a Case Study for South West Nigeria. *Energies* **2014**, *7*, 8508.
45. Obando Montaño, A. An Approach to Determine the Weibull Parameters for Wind Energy Analysis: The Case of Galicia (Spain). *Energies* **2014**, *7*, 2676–2700.
46. Keyhani, A.; Ghasemi-Varnamkhasti, M.; Khanali, M.; Abbaszadeh, R. An assessment of wind energy potential as a power generation source in the capital of Iran, Tehran. *Energy* **2010**, *35*, 188–201. [CrossRef]
47. Caballero, F.; Sauma, E.; Yanine, F. Business optimal design of a grid-connected hybrid PV (photovoltaic)-wind energy system without energy storage for an Easter Island's block. *Energy* **2013**, *61*, 248–261. [CrossRef]
48. National Renewable Energy Laboratory New Transparent Cost Data Base. Available online: https://openei.org/apps/TCDB/#blank (accessed on 3 November 2018).
49. Abreu, E.F.; Canhoto, P.; Prior, V.; Melicio, R. Solar resource assessment through long-term statistical analysis and typical data generation with different time resolutions using GHI measurements. *Renew. Energy* **2018**, *127*, 398–411. [CrossRef]
50. Zawilska, E.; Brooks, M. An assessment of the solar resource for Durban, South Africa. *Renew. Energy* **2011**, *36*, 3433–3438. [CrossRef]
51. US Energy Information Administration: Today in Energy. 2015. Available online: https://www.eia.gov/todayinenergy/detail.php?id=22832 (accessed on 5 November 2018).
52. Global Solar Atlas. Available online: https://www.globalsolaratlas.info/ (accessed on 10 November 2018).
53. Fischer, G.; Prieler, S.; Velthuizen, H; Lensink, S.M; Londo, M.; de Wit, M. Biofuel production potentials in Europe: Sustainable use of cultivated land and pastures. Part I: Land productivity potentials. *Biomass Bioenergy* **2010**, *34*, 159–172. [CrossRef]
54. Renewable Energy Cost Analysis—Biomass for Power Generation. 2012. Available online: https://www.irena.org (accessed on 12 November 2018).
55. Silva, D.A.L.; Delai, I.; Montes, M.L.D.; Ometto, A.R. Life cycle assessment of the sugarcane bagasse electricity generation in Brazil. *Renew. Sustain. Energy Rev.* **2014**, *32*, 532–547. [CrossRef]
56. Magbity, I. Prospect of Bio-fuels in Sierra Leone. Available online: https://www.grin.com/ (accessed on 10 November 2018)
57. Sierra Leone: Sugar Cane, Production Quantity. Available online: http://www.factfish.com (accessed on 12 November 2018).
58. Mohamad Izdin Hlal, A.; Ramachandaramurthya, K.V.; Sanjeevikumar, P.; Pouryekta, A.; Hamid Reza Kaboli, C.; Tuan Ab Rashid Bin Tuan Abdullah, D. NSGA-II and MOPSO based optimization for sizing of hybrid PV/wind/battery energy storage system. *Int. J. Power Electron. Drive Syst.* **2019**, *10*, 463–478. [CrossRef]
59. González, A.; Riba, J.R.; Rius, A.; Puig, R. Optimal sizing of a hybrid grid-connected photovoltaic and wind power system. *Appl. Energy* **2015**, *154*, 752–762. [CrossRef]
60. Singh, J.; Chauhan, A. Assessment of biomass resources for decentralized power generation in Punjab. *Int. J. Appl. Eng. Res.* **2014**, *9*, 869–876.
61. Kawashima, A.; Morais, M.; Martins, L.; Guerrero, V.; Abou Rafee, S.; Capucim, M.; Martins, J. Estimates and Spatial Distribution of Emissions from Sugar Cane Bagasse Fired Thermal Power Plants in Brazil. *J. Geosci. Environ. Prot.* **2015**, *3*, 72–76. [CrossRef]
62. Electricity Storage and Renewables (2017): Costs and Markets to 2030. Available online: https://www.irena.org (accessed on 10 November 2018).
63. Cost estimates for Thermal Peaking Plants (2008): Parsons Brinckerhoff New Zealand Ltd. Available online: https://www.electricitycommission.govt.nz (accessed on 12 November 2018).
64. Emission Factors for Greenhouse Gas Inventories (2018): Parsons Brinckerhoff New Zealand Ltd. Available online: https://www.epa.gov (accessed on 15 November 2018).
65. CO2 Emission Factors for Fossil Fuels. Available online: https://www.umweltbundesamt.de/en/publikationen/co2-emission-factors-for-fossil-fuels (accessed on 15 November 2018).

66. Khiareddine, A.; Ben Salah, C.; Rekioua, D.; Mimouni, M. Sizing methodology for hybrid photovoltaic /wind/hydrogen/battery integrated to energy management strategy for pumping system. *Energy* **2018**, *153*, 743–762. [CrossRef]
67. Daniel M. Kammen, K.K.; Fripp, M. Putting Renewables to Work: How Many Jobs Can the Clean Energy Industry Generate? *Energy Policy* **2010**, *38*, 919–931.
68. Singh, V.; Fehrs, J. The Work That Goes Into Renewable Energy. 2001. Available online: http://www.globalurban.org (accessed on 5 August 2018).